This article was downloaded by:[University of Washington]
On: 13 March 2008
Access Details: [subscription number 758876551]
Publisher: Taylor & Francis
Informa Ltd Registered in England and Wales Registered Number: 1072954
Registered office: Mortimer House, 37-41 Mortimer Street, London W1T 3JH, UK

International Reviews in Physical Chemistry
Publication details, including instructions for authors and subscription information:
http://www.informaworld.com/smpp/title~content=t713724383

Applications of single-molecule microscopy to problems in dyed composite materials

Kristin L. Wustholz [a]; Daniel R. B. Sluss [a]; Bart Kahr [a]; Philip J. Reid [a]
[a] Department of Chemistry, University of Washington, Seattle, WA 98195-1700

First Published on: 06 February 2008
To cite this Article: Wustholz, Kristin L., Sluss, Daniel R. B., Kahr, Bart and Reid, Philip J. (2008) 'Applications of single-molecule microscopy to problems in dyed composite materials', International Reviews in Physical Chemistry, 1 - 34
To link to this article: DOI: 10.1080/01442350701819438
URL: http://dx.doi.org/10.1080/01442350701819438

PLEASE SCROLL DOWN FOR ARTICLE

Full terms and conditions of use: http://www.informaworld.com/terms-and-conditions-of-access.pdf

This article maybe used for research, teaching and private study purposes. Any substantial or systematic reproduction, re-distribution, re-selling, loan or sub-licensing, systematic supply or distribution in any form to anyone is expressly forbidden.

The publisher does not give any warranty express or implied or make any representation that the contents will be complete or accurate or up to date. The accuracy of any instructions, formulae and drug doses should be independently verified with primary sources. The publisher shall not be liable for any loss, actions, claims, proceedings, demand or costs or damages whatsoever or howsoever caused arising directly or indirectly in connection with or arising out of the use of this material.

International Reviews in Physical Chemistry
2008, 1–34, iFirst

Taylor & Francis
Taylor & Francis Group

Downloaded By: [University of Washington] At: 18:07 13 March 2008

Applications of single-molecule microscopy to problems in dyed composite materials

Kristin L. Wustholz, Daniel R.B. Sluss, Bart Kahr and Philip J. Reid*

Department of Chemistry, University of Washington, Box 351700, Seattle WA 98195–1700

(*Received 28 September 2007; final version received 19 November 2007*)

Recent progress in single-molecule spectroscopy of dyed composite materials is reviewed. In particular, single-molecule studies of dyed polymer films and dye inclusion crystals are described that seek to understand local guest–host interactions and environmental heterogeneity. Single-molecule orientational studies of chromophores in polymer films and mixed crystals are discussed with particular relevance to materials and device applications. Studies of single-molecular reorientational dynamics in polymers in the presence of an electric field designed to establish alignment are described. Static orientational measurements in mixed crystals, wherein alignment is a consequence of crystal growth, reveal a surprisingly wide distribution of molecular orientations. Moreover, the complex photophysics of single molecule in anisomorphous mixed crystals are explored and described in the context of environmental heterogeneity and distributed kinetics. The emerging literature regarding dispersed kinetics observed for individual emitters (e.g. quantum dots, single molecules in polymers, etc.) is reviewed. Finally, the outlook of single-molecule spectroscopy in dye-doped materials is outlined.

Contents

		PAGE
1.	**Introduction**	2
2.	**Molecular orientation in dyed composite materials**	3
	2.1. Dyed polymer composites	3
	2.2. Static and dynamic orientation in chromophore-polymer composite materials	5
	2.3. Dyed crystals	9
	2.4. Single-molecule measurements of molecular alignment	11
	2.5. Static alignment in dyed salt crystals	12
3.	**Single-molecule photophysics in dyed composite materials**	16
	3.1 Single-molecule photophysics in dyed salt crystals	19
	3.2. Power-law blinking behaviour in individual molecules	22

*Corresponding author. Email: preid@chem.washington.edu

ISSN 0144-235X print/ISSN 1366-591X online
© 2008 Taylor & Francis
DOI: 10.1080/01442350701819438
http://www.informaworld.com

Downloaded By: [University of Washington] At: 18:07 13 March 2008

3.3. Distributed kinetics models 22
3.4. Role of the environment in power-law behaviour 24
3.5. The origin of distributed kinetics in chromophores 26
3.6. Memory in single-molecule emission 28

4. Summary 31

Acknowledgements 31

References 31

1. Introduction

The electronic absorption and emission spectra of organic chromophores in condensed environments possess information concerning molecular structure and dynamics. However, these spectra are generally broad and featureless due to inhomogeneous broadening created by a distribution of local environments. To circumvent this complication, spectroscopists have developed techniques to obtain high-resolution molecular spectra in condensed phases. Well-resolved vibronic spectra were first obtained in the 1930s on single crystals of aromatic hydrocarbons (e.g. benzene, naphthalene) at low temperatures [1,2]. Two decades later, low-temperature studies of aromatic hydrocarbons in solids (i.e. Shpol'skii matrices and crystals) provided the first quasi-line spectra of organic compounds [3]. For example, Shpol'skii discovered that aromatic hydrocarbons dissolved in *n*-paraffins exhibited fine-structured spectra at low temperatures corresponding to zero phonon transitions. In the 1970s, hole burning [4–6] and fluorescence line narrowing [7,8] techniques were developed that utilize selective excitation to investigate the individual components of an inhomogeneous molecular distribution.

Although energy-selective spectroscopic techniques and low-temperature matrix-isolation methods can minimize inhomogeneous broadening, the ultimate limit is provided by single-molecule spectroscopic techniques. Lange and coworkers approached the single-absorber limit ($N \leq 5$) by studying the inherent, low-temperature statistical fine structure of Sm^{2+} ions in CaF_2 crystals [9]. However, true single-molecule resolution was not achieved until Moerner and Kador performed low-temperature studies of pentacene substituted into crystals of *p*-terphenyl [10]. In these seminal studies, hidden heterogeneities in molecular photophysics were observed, and this work demonstrated the utility of single molecules as 'nanoreporters' of local guest–host environments in condensed media [11–13]. Motivated by these studies, the spectroscopy of individual organic molecules in condensed environments has seen substantial growth. Advantages of this approach include minimization of ensemble-averaging, environmental heterogeneity, and non-synchronicity (particularly advantageous for studies of biomolecules). Furthermore, single-molecule studies have revealed a multitude of previously unobserved phenomena (e.g. quantum jumps [14], photon antibunching [15], etc.).

Single-molecule spectroscopy is by now a well-established field, and the techniques employed have been reviewed in detail [16–20]. Instead, we focus here on the application of single-molecule techniques to problems in materials chemistry. For example, single-molecule measurements have been applied to systems with novel device applications

Downloaded By: [University of Washington] At: 18:07 13 March 2008

such as high-speed telecommunications [21] and quantum computing [22]. An emerging class of materials for next-generation electro-optic (EO) switches are polymers containing oriented dye molecules having a large first hyperpolarizability. These materials hold the promise of information transmission at larger bandwidths and lower operational voltages as compared to inorganic devices (i.e. $LiNbO_3$) [23]. However, a crucial issue facing these materials is the successful translation of molecular systems of large hyperpolarizabilities into macroscopic assemblies that have a similarly large EO activity [24,25]. Bulk nonlinear optical activity requires non-centrosymmetry [26], a condition that is typically met by placing an electric or 'poling' field across the dye-doped polymer to induce chromophore alignment. However, theoretical work suggests that poling is only partially effective in achieving molecular alignment [27]. Consequently, if the goal is to enhance the EO efficiency of these materials, then a detailed understanding of the poling process must be acquired. Whereas ensemble-averaged spectroscopy provides an average value of molecular orientation, single-molecule microscopy can examine the nanostructures of dye-doped polymeric systems, providing molecular-level information on how single molecule orientation and molecular interactions impact EO device efficiency.

Molecular orientation can also be established by the host matrix. For example, in isomorphous mixed crystals chromophore alignment is achieved by direct substitution of guests into non-equivalent lattice sites of the host [28,29]. Since local heterogeneity in the crystal is minimal with respect to that in polymer films, investigating the extent of molecular orientation in mixed crystals represents the optimal approach for minimizing inhomogeneous broadening. Furthermore, single-molecule studies of these structurally-defined systems can provide a deeper understanding of molecular photophysics including blinking dynamics, the nature of non-emissive states, and photodecomposition pathways. This review focuses on the physical principles, methods, and results of single-molecule studies of organic luminophores in condensed environments with particular relevance to materials and device applications (e.g. single-photon sources, organic based EO modulators). We discuss the application of single-molecule studies in polymer films and dye inclusion crystals to understanding local guest–host interactions and environmental heterogeneity of the surrounding matrix.

2. Molecular orientation in dyed composite materials

2.1. *Dyed polymer composites*

Polymers are complex, dynamic materials with properties that vary widely as a function of composition and temperature. For example, near the glass transition temperature (T_g) of a polymer the bulk viscosity can change by orders of magnitude over just a few degrees [30]. Polymer dynamics have been studied for over 50 years [30–35] and research continues toward understanding these complex materials. One method by which to study these environments is to use single dye molecules as reporters of local structure and dynamics [36–41]. In particular, the reorientational dynamics of dyes embedded in polymer films have been studied in order to probe environmental heterogeneity [39,42], relaxation dynamics of the host, [38,43] and polymer viscosity [44]. Single-molecule reorientation

Downloaded By: [University of Washington] At: 18:07 13 March 2008

studies of the rhodamine analogue 5-TRITC in poly(methyl acrylate) (PMA) were performed using polarization-sensitive wide-field microscopy [39]. Single molecules exhibited dispersed rotational dynamics above and near the glass transition temperature, demonstrating the heterogeneity of the host environment. Spatial heterogeneity and polymer relaxation dynamics in poly(methyl methacrylate) (PMMA) films have been studied using single $DiIC_{18}$ molecules [38]. Here, the authors determined that probe molecular dynamics are governed by polymer motions resulting from α relaxations in the glassy state of the host [38]. Molecular reorientation can also be quantified by measuring orientation over time and collecting the distribution of first-jump times [45]. For example, the distribution of $DiIC_{18}$ molecules that reoriented as a function of time in poly(vinylbutyral) (PVB) was fit to a stretched exponential function, consistent with a distribution of host environments caused by thermal fluctuations. Other means by which to garner information about the host environment have included measurements of single-molecule blinking dynamics [46] and lifetimes [47,48].

Chromophore reorientation is critical to functional EO chromophore-polymer composites. Chromophore-doped polymers are typically centric obviating EO activity [27]. When processing these materials, chromophore order (i.e. non-centrosymmetry) is achieved during the 'poling' process. In poling, an external electric field (E) is applied to the composite material at temperatures near the T_g of the polymer host. The chromophore dipole moment (μ) interacts with the external field to induce ordering, then the system is cooled to preserve the field-induced chromophore alignment. The extent of EO activity is related to the product of chromophore molecular hyperpolarizabilty (β), chromophore number density (N), and the extent of poling-induced molecular order [26]: $EO \propto N\mu\beta\langle\cos^3\theta\rangle$. The orientational term, $\langle\cos^3\theta\rangle$, corresponds to the angle between the molecular transition electric dipole moment and the direction of the external field. This equation demonstrates that one strategy for optimizing EO activity in dyed-polymer composites is to maximize the extent of molecular order; therefore, understanding the details of molecular reorientation in a polymer host is a critical step toward the development of polymer-based EO devices.

Second-harmonic generation (SHG) has been used to study order in chromophore-polymer composite materials. In particular, SHG has been used to probe poling efficiency, and to optimize experimental parameters in the poling process. Singer *et al*. [49] studied corona poling efficiency using SHG, and later experiments [50] demonstrated that stacked or in-plane electrode geometries were sufficient to achieve non-centrosymmetry. Bulk SHG measurements on poled polymers demonstrated that as the temperature is decreased relative to T_g, more chromophore order is retained in the system after the poling field is removed [51]. Chromophore ordering in dye-doped polymer films has been investigated using scanning SHG where micron-sized spatial heterogeneities were observed [52]. By adding polarization sensitivity to scanning SHG measurements, Le Floc'h *et al*. [53] determined the average orientation of these domains. Although these ensemble-averaged experiments provided evidence that poling can achieve molecular alignment, the extent and efficiency of chromophore ordering in these systems is still an area of debate [21,27,54]. Single-molecule spectroscopy can examine the nanostructures of dye-doped polymer systems, providing molecular level information on single-molecule orientations, local environmental heterogeneity, and how molecular interactions impact EO device efficiency.

Downloaded By: [University of Washington] At: 18:07 13 March 2008

2.2. *Static and dynamic orientation in chromophore-polymer composite materials*

Several single-molecule studies have explored two- and three-dimensional order of guest molecules in polymer hosts [55–59]. Weston *et al.* measured the two-dimensional static orientations and reorientational dynamics of dyes in a polymer matrix using polarization-modulation confocal microscopy [45]. Individual molecules exhibited discrete jumps in orientation, and the reorientational dynamics depended on film thickness consistent with a combination of thermal and photoinduced reorientation mechanisms. Using widefield microscopy, single-molecule orientations of the dye 5-TRITC in PMA were measured, and a broad distribution of orientations was observed [39]. In addition to confocal and standard wide-field microscopies, TIR has been used to monitor the rotational dynamics of single molecules in polymer films. For example, TIR was used to probe the nanoscale environmental heterogeneity and relaxation dynamics of dyes within the glassy state of a PMA host [38].

We have used fluorescence excitation dichroism to study the effect of an applied electric field on molecular orientation during poling of chomophore-polymer composite materials [21,54]. During the poling process, the potential created by the interaction of the electric field with the molecular dipole moment is expected to bias the molecular-orientational distribution towards the direction of the electric field. The alignment potential depends on the product of the molecular dipole moment and the applied field. For example, the model nonlinear optical chromophore, DCM, possesses a dipole moment of ~10 D, and in the presence of 50 V/μm fields generally employed in processing of these materials a potential of $\sim 1.7 \times 10^{-21}$ J is achieved. The orientational distribution is governed by the Boltzmann probability distribution that depends on the ratio of electric-field induced potential in relation to the amount of thermal energy available to the system, kT, where k is Boltzmann's constant, and T is temperature. In the DCM studies, this ratio was 0.4 demonstrating that the thermal energy available is greater than field-induced potential. This simple calculation begs the question: just what is the extent of the perturbation created by the presence of the electric field on molecular orientation?

Fluorescence images from single DCM molecules dispersed in PMA and placed between two electrodes are presented in Figure 1 [21]. The 300-nm diameter of the molecular images reflects the near-diffraction limited focus of the laser. Single molecules were located by performing a raster scan of the sample until a molecule was located and the flourescence dichroism was measured as a function of time. Figure 2 illustrates the analysis required to connect the time-dependent fluorescence dichroism to molecular rotation. Anticorrelations in intensities between dichroic components of the emission are observed consistent with molecular rotation, until permanent loss of the signal occurs due to photodestruction (Figures 2a and 2b). Using $I_{\parallel}(t)$ and $I_{\perp}(t)$, the reduced dichroism ($A(t)$) is calculated by normalizing the difference between the two orthogonal components by their sum [21,54] as presented in Figure 2c. Finally, the autocorrelation of $A(t)$, $C(t)$, is determined and analyzed as shown in Figure 2d. The decay of $C(t)$ is not well described by a single exponential as illustrated by the mismatch between the exponential fit (dashed line) and data (black diamond). In contrast, the data are better fit by the stretched exponential function (solid line). The fitting parameters reported for the stretched exponential are the stretching parameter (β_{KWW}) and the weighted average correlation time (τ_c) [21]. Previous studies

Downloaded By: [University of Washington] At: 18:07 13 March 2008

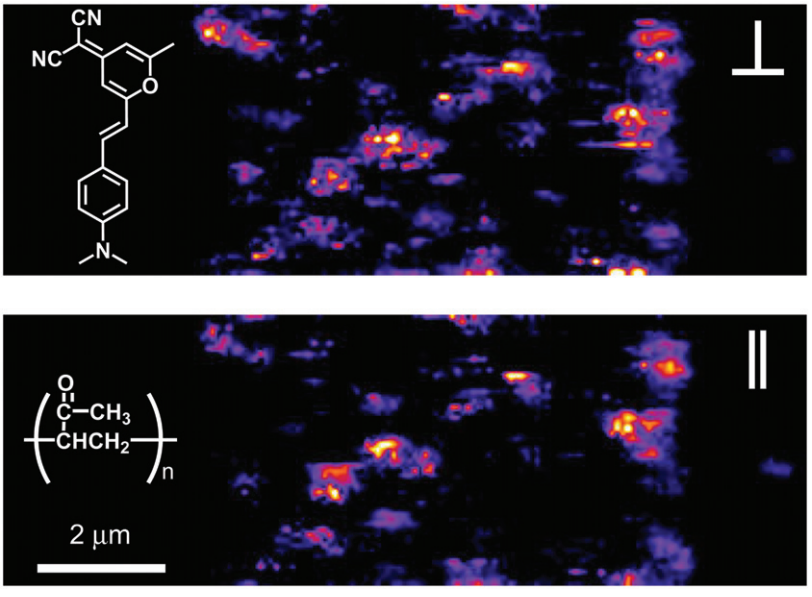

Figure 1. False-colour images of the flourescence of single DCM molecules. The figure represents a $5 \times 5\,\mu m^2$ scan employing 0.1 mm steps of 10^{-9} M DCM in 15 wt% PMA. The fluorescence is polarized parallel to the applied electric field (top) or perpendicular (bottom). The colour scale corresponds to 300 to 50 counts per 100 ms.

have demonstrated that the rotational dynamics of single molecules in polymer hosts exhibit stretched-exponential behaviour associated with a heterogeneous polymer environment [36,39,45]. For example, studies of $DiIC_{18}$ in polymer films demonstrated that single-molecule rotational dynamics, evidenced by the percentage of molecules that reoriented over time, are well represented by stretched exponential functions consistent with thermal-induced environmental fluctuations in the host environment [45]. In addition, the autocorrelation of the reduced dichroism for single molecules of 5-TRITC in PMA were fit by stretched exponential functions [39].

Histograms of β_{KWW}, τ_c, and the time-averaged ratio of $\langle I_{\parallel} \rangle$ to $\langle I_{\perp} \rangle$ for DCM molecules in PMA in the presence and absence of a 50 V/μm electric field are shown in Figure 3. The deviation of β_{KWW} from 1 (Figure 3a) suggests the rotational dynamics reflect the heterogeneous environment of the polymer host. However, the preponderance of β_{KWW} values lie between 0.7 and 1 demonstrating that the rotational environment is not far from homogeneous. Probe-specific rotational dynamics may be responsible for the differences in the varying degree of exponential decay of $C(t)$ between studies [21,39,54]. Wang and Richert have recently demonstrated that for probe molecules in glass forming liquids, if the rotational time constant of the probe is significantly greater than the structural relaxation time of the surrounding environment, the rotational dynamics of the probe will demonstrate exponential decay [60]. The near-exponential decay of molecular rotational correlation [21,54] may reflect the rapid fluctuations of the polymer host relative to the slower rotational dynamics of the probe or be due to limited sampling of the molecular ensemble.

Downloaded By: [University of Washington] At: 18:07 13 March 2008

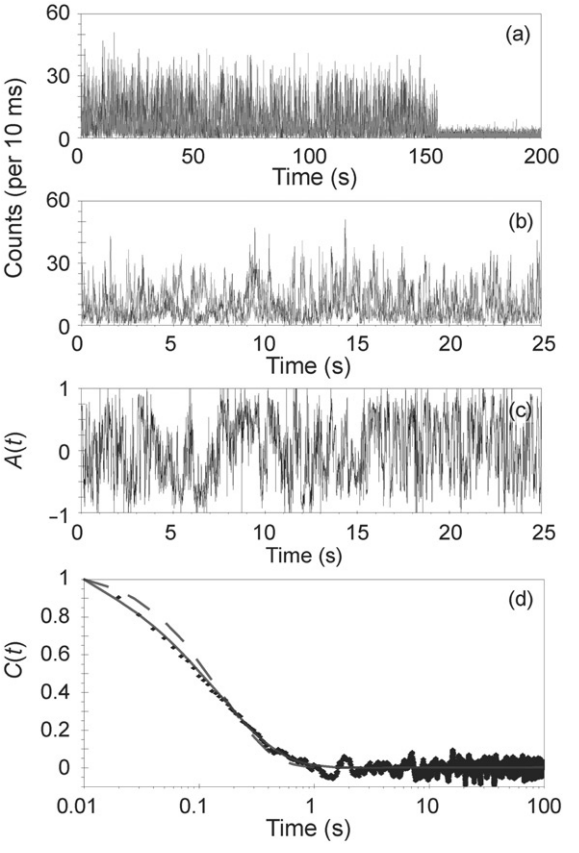

Figure 2. A typical single molecule time trace of DCM in PMA ($T_g = 11°C$). Panel A presents the signal for the two polarization components of the fluorescence ($\|$ to the electric field as light grey, $\perp$ as dark grey). A single-step bleach at 150 s is observed, consistent with single-molecule photodestruction. In panel B, the first 25 s of the evolution in panel A is shown to more clearly depict the rotational dynamics. The reduced linear dichrosim, $A(t)$, is illustrated in panel C. Panel D is a fit to the autocorrelation of the transient showing both an exponential fit (dashed, $\tau = 0.16$ s) and a fit to a stretched exponential function (solid, $\tau_{KWW} = 0.15$ s and $\beta_{KWW} = 0.78$).

The effect of an external electric field on the rotational dynamics of DCM (τ_c) was determined by comparing the weighted average correlation times for molecules in the presence and absence of the external field as seen in Figure 3b. Although the histograms with and without the external field are similar, a shift to higher τ_c values is observed in the presence of the poling field, suggesting that the rotational dynamics are retarded in the presence of the electric field. An alternate way to gauge the effect of an applied field is illustrated in Figure 3c. Here, histograms of the ratio of $\langle I_{\|} \rangle$ to $\langle I_{\perp} \rangle$ with averaging over the defined molecular lifetime are shown. The application of the poling field is expected to bias the molecular alignment in the direction of the field; therefore, this should be reflected by an increase in the dichroic ratio in the presence of the electric field. The average intensity ratio is 0.98 ± 0.02 with no external field, and in the presence of a 50 V/μm field the average ratio undergoes a sight increase to 1.00 ± 0.03. In addition, the histogram

Downloaded By: [University of Washington] At: 18:07 13 March 2008

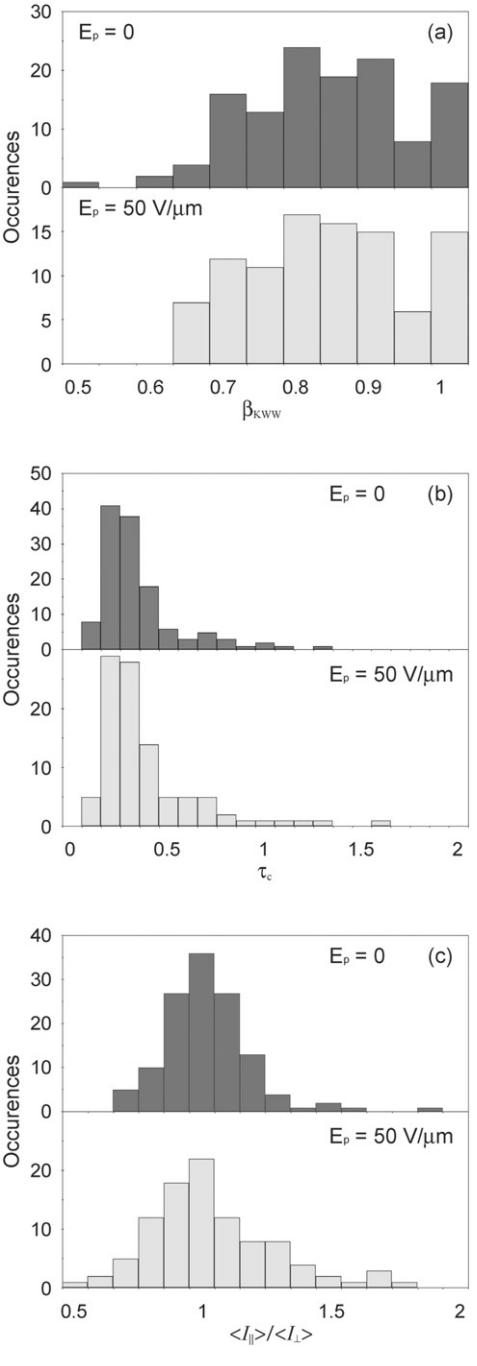

Figure 3. Histograms for the single-molecule correlation time (τ_c panel A) fit parameter (β_{KWW} panel B), and $\langle I_{\parallel}\rangle/\langle I_{\perp}\rangle$ (panel C) for DCM are shown. The values with no perturbation are shown on top of each panel, and on the bottom are values in the presence of a 50 ± 5 V/μm electric field.

Downloaded By: [University of Washington] At: 18:07 13 March 2008

in the presence of the electric field demonstrates broadening and skewing of the intensity ratio to values greater than unity and is consistent with a biasing of the molecular orientation in the direction of the electric field.

These results demonstrate that DCM molecules in PMA experienced significant rotational mobility when $T > T_g$. The molecular rotational dynamics of DCM are only slightly perturbed by the presence of a 50 V/μm electric field, which is representative of typical fields employed in device construction. Given a poling field of this magnitude and the dipole moment of DCM (10 D), μE is approximately equal to $0.4\,kT$. Therefore, the amount of thermal energy available to DCM is significantly greater than the electrostatic potential energy created by the poling field. This energetic comparison is consistent with the observation that the poling field provides only a modest perturbation to the rotational dynamics of DCM [21].

2.3. *Dyed crystals*

Until recently, single-molecule studies on mixed crystals were limited to classic systems where host and guest molecules are of similar size and shape, consistent with Mitscherlich's principle of isomorphism [61]. Naturally, the appeal of single-molecule studies in mixed crystals relative to other condensed-phase hosts is the definition, periodicity, and stabilization provided by the crystal lattice. The corresponding disadvantage: mixed crystals with isomorphous components are traditionally difficult to grow and handle, examined at extremely low temperatures, and limited to a modest number of aromatic hydrocarbon dopants (e.g. pentacene, perylene, terrylene). However, there exist classes of mixed crystals with *an*isomorphous components containing robust luminophores (e.g. rhodamines, fluoresceins) that possess significant advantages over classic mixed-crystal systems [62]. For example, single crystals of potassium acid phthalate [63–66] and potassium sulphate [67,68] are easily grown from aqueous solution at room temperature in the presence of many luminophores. We have explored mixed crystals with *an*isomorphous components, crystals observed but oddly overlooked for over a century, in contemporary studies of single-molecule alignment and photophysics.

As is well-known, many crystals are coloured due to traces of foreign matter. Colourless and inexpensive Al_2O_3 crystals become rose-coloured sapphires, valuable to jewellers and laser spectroscopists when titanium ions are present in the host lattice. In contrast, we are less familiar with the dyeing of crystals using complex organic chromophores that are chemically and structurally dissimilar from the host. The scientific study of dyeing crystals with chromophores that are anisomorphous with the host was initiated in the mid-nineteenth century by Sénarmont who discovered that solutions of $Sn(NO_3)_2 \cdot 4H_2O$ containing logwood extract deposited crystals that were red or violet depending on the orientation of the crystal with respect to the plane of incident linearly polarized light [62]. Although many crystallographers struggled in vain [69] to reproduce the mixed crystal thereafter referred to as Sénarmont's salt, other examples of dye inclusion crystals were obtained along the way (e.g. Congo red in sugar [70] and crystal violet in poppy acid crystals [71]) in which dyes recognized a specific facet of the growing crystal to produce single crystals with dyed regions that resemble hourglasses, Maltese crosses, hillocks, and more. A detailed review of the history of dyeing crystals as well as catalogues of

Downloaded By: [University of Washington] At: 18:07 13 March 2008

dye inclusion crystals that are easily grown from evaporation of simple salt solutions appears elsewhere [62].

From the time of Sénarmont's discovery until the 1940s, the crystallographic literature contained sporadic discussions on the origins of linear dichroism in dye inclusion crystals as well as dyed crystal growth and habit modification. For instance, how were mixed crystals with *an*isomorphous components able to accommodate such obtrusive impurities? Tammann demonstrated that under conditions of supersaturation far from equilibrium, solutions of simple salts can subvert the principle of isomorphism, depositing crystals that have oriented and overgrown anisomorphous guests [72]. Interestingly, the emergence of high-resolution spectroscopy in condensed phase during the 1930s corresponded with the last comprehensive studies on dye inclusion crystals. In this review, we describe our efforts to reunite mixed crystals with single-molecule spectroscopy in order to inform contemporary studies on the photophysical and orientational properties of dyed composite materials.

By exploring dyed crystals of the past, we have discovered several hosts [62] such as potassium acid phthalate [62–66,73] (KAP, space group $Pca2_1$, $a = 9.614$ Å, $b = 13.330$ Å, $c = 6.479$ Å [75]) that show remarkable tolerance for dyes of varying size, shape, and chemical affinities. In particular, we have demonstrated that KAP incorporates chromophores such as rhodamines, [65,66] acridines, [63,64] nonlinear optical molecules, [65,66] and triphenylmethane dyes [73]. In addition to its remarkable acceptability for guest molecules, KAP is easily grown from aqueous solution as large {010} plates, with perfect cleavage parallel to these faces. During growth from solution, guest molecules are differentially adsorbed and overgrown by faces of KAP not related by symmetry, a phenomenon called *inter*sectoral zoning, illustrated by DCM (4-dicyanomethylene-2-methyl-6-*p*-dimethylaminostyryl-4H-pyran) in the $\{11\bar{1}\}$ growth sector of KAP (Figure 4). *Intra*sectoral zoning is observed when dye impurities inhomogeneously deposit *within* a single growth sector. For instance, in the low supersaturation regime, the KAP crystal surface propagates through screw dislocations that produce growth hillocks, shallow stepped pyramids with non-equivalent vicinal slopes that express distinct affinities for additives. Violamine R (VR) and 2′,7′-dichlorofluorescein (DCF) recognize the {010} growth sector of KAP (i.e. intersectoral zoning) and within this volume only the fast slopes of growth hillocks (i.e. intrasectoral zoning) that are revealed as luminescent chevrons (Figure 4). These results express the highly specific deposition of dyes into a crystal host, and show that dye inclusion crystals provide opportunities to study alignment and photophysics of single molecules.

In addition to the specific chemical zoning observed in dyed KAP crystals, linear dichroism measurements demonstrate that single-crystal matrix isolation provides an efficient orientation mechanism for included dyes. The projected transition dipole moment orientation (θ) of a fluorophore can be obtained by measuring the absorption or emission dichroism. For example, the polarized excitation dichroism following 488-nm illumination in DCM-dyed KAP crystals revealed an average dye orientation of 31.0° from [100] in the *ac*-plane. Average dye alignment in VR-dyed KAP is roughly 45° from [100]. Although these examples demonstrate that dyes are oriented in KAP crystals, the extent to which overgrowth by the crystal lattice results in chromophore alignment is a question that only single-molecule techniques are capable of addressing. For instance, does an average orientation for VR in KAP of 45° correspond to a narrow or broad orientational

Downloaded By: [University of Washington] At: 18:07 13 March 2008

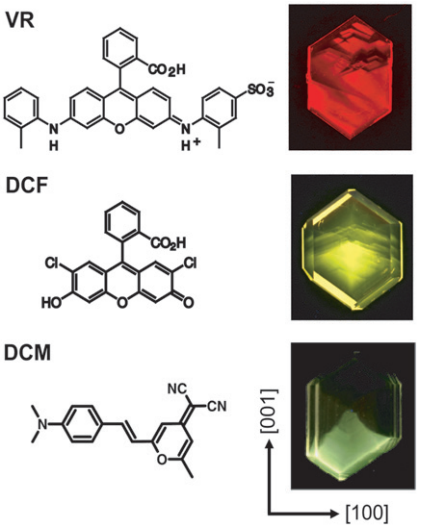

Figure 4. Dye-inclusion KAP crystals. Violamine R (VR) and 2′7′-dichlorofluorescein (DCF) are included on the fast slopes of growth hillocks within the {010} growth sector of KAP. DCM is incorporated into the $\{11\bar{1}\}$ sector of KAP.

distribution centred at 45°, or rather, an isotropic distribution of dyes? Moreover, the astonishing generality with which KAP crystals can orient and overgrow functional dyes argues that dyed crystals have been overlooked as photonic materials [65,76]. Comparison to polymers at the single-molecule level will firmly establish the differences in alignment and macroscopic efficiency that are a consequence of two distinct mechanisms: poling of polymers and growth anisotropy in crystals.

2.4. *Single-molecule measurements of molecular alignment*

The polymer-composite and mixed-crystal studies described above require the ability to ascertain molecular orientation; therefore, we first focus on the ability of single-molecule techniques to determine molecular order in two and three dimensions. The distribution of molecular orientations in a host matrix can reveal the extent of alignment that is a result of environmental heterogeneity and local guest–host interactions. Generally, polarized light is employed to determine the orientation of molecular transition dipole moments [77]. In the first single-molecule polarization-sensitive experiments, Güttler *et al.* [28,29] measured the fluorescence signal of single pentacene molecules in *p*-terphenyl as a function of linear excitation polarization, and fit the resulting curve to a sinusoidal modulation in order to determine the transition dipole moment orientation. Polarization-modulation spectroscopy has also been used to measure single-molecule orientations in stretched polyethylene films containing terrylene [78]. A more common approach is to determine the two-dimensional orientation (θ) of a fluorophore by measuring the absorption or emission intensity following linearly-polarized excitation along two orthogonal directions ($I_{\parallel}/I_{\perp}$) according to [77,79]: $\theta = \tan^{-1}\sqrt{I_{\parallel}/I_{\perp}}$. A significant complication in this approach is that the high-NA objectives employed can present a large half-aperture angle resulting in

Downloaded By: [University of Washington] At: 18:07 13 March 2008

'*z*-mixing' of the excitation of transition dipole moments orientation orthogonal to the *xy*-plane. This effect precludes measurement of the orientational extremes [77,79]. A simple approach to measuring the extent of *z*-mixing is to repeat the orientation measurements using a lower-NA objective. For example, our orientation measurements of VR in KAP demonstrated essentially no change between a 1.3- and 0.8-NA objective suggesting that *z*-mixing was modest in these experiments [66]. Molecular orientation studies in mixed crystals have also been performed using total internal reflection (TIR) microscopy. However, this method is limited to molecules located near the surface of the material of interest. For example, in ultrathin samples of *p*-terphenyl doped with terrylene, TIR measurements revealed that single molecules were aligned normal to the plane of the spun coat crystalline film [80]. Single-molecule measurements of alignment in projection have also been performed in polymers [81], on glass surfaces [82,83], in Shopol'skii matrices [84,85] and sol–gel environments [86].

More recently, three-dimensional (3D) measurement techniques (e.g. annular illumination, radially-polarized illumination, etc.) were developed and applied to single molecules [58,81] as well as individual semiconductor quantum dots [87]. For example, the orientation and location of both chromophores in a Forster resonance energy transfer (FRET) pair were measured in three dimensions using annular illumination with two excitation wavelengths [88]. The FRET pairs were tethered together using a rigid molecular bridge and the authors observed a distribution of pair orientations, illustrating that the relative geometry of the embedded chromophores is determined by the polymer host environment. The 3D orientations of four-chromophore dendrimers doped into thin polymer films were determined using wide-field defocusing, and in conjunction with fluorescence lifetime measurements, were used to validate the energy hopping properties of the multichromophoric system [89].

2.5. *Static alignment in dyed salt crystals*

Soon after the achievement of single-molecule resolution, Güttler *et al*. [28,29] performed the first comprehensive studies on single-molecule alignment in mixed crystals. In particular, the transition-dipole-moment orientations of single pentacene molecules in crystals of *p*-terphenyl were measured using polarization modulation. As expected for an isomorphous host/guest pair, pentacene molecules substituted into four non-equivalent sites in the *p*-terphenyl lattice in relatively narrow orientational distributions [28]. More recent orientation studies in mixed crystals were performed at room temperature on terrylene molecules doped into ultrathin samples of *p*-terphenyl, where terrylene molecules aligned normal to the plane of the spun-coat crystalline film [80]. In addition, Moerner and Werley [90] demonstrated that terrylene molecules existed in two subpopulations within crystalline films of *p*-terphenyl obtained from spin coating. One population of molecules was photostable, oriented, and immobile, while the other was mobile, tracking the crystalline defects over distances on the order of microns. In recent decades, single-molecule studies of alignment in mixed crystals have taken a backseat to measurements in other condensed environments (e.g. polymer films) since traditional mixed crystals are difficult to prepare and are limited to a modest number of simple aromatic dopants. In the following section, we describe our efforts to study single-molecule orientations in mixed crystals containing complex luminophores, unrestricted by host/guest isomorphism.

Downloaded By: [University of Washington] At: 18:07 13 March 2008

To develop a molecular-level understanding of how the rhodamine derivative violamine R (VR) is oriented in the KAP crystal host, single-molecule measurements were performed [66,91]. Anisomorphous mixed crystals are hereafter referred to as host/guest (e.g. violamine R-dyed potassium acid phthalate is KAP/VR). Figures 5a and 5b show a typical dataset, consisting of fluorescence images from KAP/VR grown from a solution containing 5×10^{-9} M dye, with images corresponding to excitation along the [100] and [001] eigenmodes of the crystal. Molecules that are brighter with excitation polarization parallel to [100] and [001] have absorption dipole moments oriented closer to the *a*- and *c*-direction, respectively. The transition dipole moment orientations of included dye molecules were determined using polarized excitation measurements. Transition dipole moment orientations (θ) were computed according to: $\theta = \tan^{-1}(1.12 \cdot DR)^{-1/2}$, where the dichroic ratio ($DR = I_a/I_c$) is corrected for the KAP birefringence [77,92]. Reported values of θ are defined with respect to [100] in the *ac*-plane. The intrinsic error in θ (the orientation of an individual dye molecule relative to the host lattice), determined by the emission fluctuations of a single-molecule time-trace, was approximately $\pm 5^\circ$.

From the measured dichroism in several KAP/VR samples, the average orientation for 200 molecules was determined to be $41.6 \pm 14.0^\circ$ (standard deviation from the mean), in agreement with the bulk measurement. However, the distribution of orientations was substantial, with a FWHM (full-width half-maximum) of $\sim 30^\circ$ and individual values ranging from 8.1° to 74.2° relative to [100] (Figure 5c). Considering the intrinsic organization present within a single crystal, and our observations of chemical zoning in heavily-dyed crystals, this result was surprising. To explore the role of conformational flexibility on alignment, we performed experiments on 2′,7′-dichlorofluorescein (DCF) incorporated into KAP. This chromophore is structurally analogous to VR, but lacks the terminal aryl rings. For single-molecule experiments employing 405-nm excitation, the average orientation of 180 molecules in KAP/DCF was found to be $42.6 \pm 18.3^\circ$ from [100] with values ranging from 5.8 to 86.5° (Figure 6). The single-molecule measurements were repeated using 532-nm excitation in order to rule out photoselection. With 532-nm excitation, the average orientation for 151 molecules in KAP/DCF was found to be $38.6 \pm 15.5^\circ$ from [100] with the orientational distribution ranging from 9.3 to 70.9° (Figure 6). The FWHM of the orientational distributions following 405-nm and 532-nm excitation were $\sim 55^\circ$ and $\sim 50^\circ$, respectively. These results demonstrate that single molecules are poorly aligned in the crystal host, despite the fact that heavily-dyed crystals demonstrate specific chemical zoning that directs dyes to the fast slopes of growth hillocks. The persistent difference between the average orientation from bulk and single-molecule measurements in KAP/DCF was found to be a consequence of anisotropic kink-site recognition [93].

We have also investigated KAP dyed with the nonlinear optical dye DCM. Heavily-dyed KAP/DCM crystals exhibit a visible absorbance spectrum with maxima at 408 nm, 432 nm, and 460 nm, and emission at 470 nm, 507 nm, and 545 nm. The fluorescence profile of the dyed crystal demonstrates a hypsochromic shift relative to solution, consistent with protonation of DCM as verified by EPR measurements. The orientations for 75 molecules of DCM in KAP were determined by polarized excitation anisotropy measurements using 488-nm excitation, and an average orientation of $33.6 \pm 7.8^\circ$ from [100] was observed, in agreement with bulk measurements. However, DCM also exhibits a wide range of chromophore orientations in the crystal, from 20.9° to 50.8° from [100].

Downloaded By: [University of Washington] At: 18:07 13 March 2008

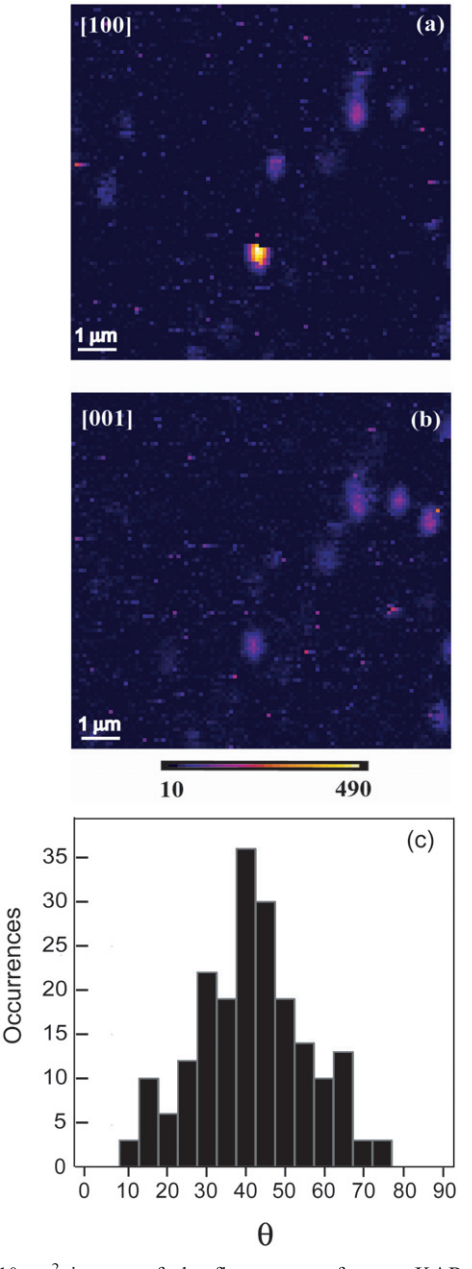

Figure 5. False-colour $10 \times 10\,\mu m^2$ images of the fluorescence from a KAP crystal grown from roughly 5×10^{-9} M VR, obtained from 532-nm excitation along orthogonal eigenmodes, (a) [100] and (b) [001]. Colour scale corresponds to counts per 100 ms. (c) Resulting histogram (bin size = 5°) of VR orientations for 200 violamine R molecules, measured as an angle between 0° and 90° from [100]. The average orientation was found to be $41.6 \pm 14.0°$ from [100].

Downloaded By: [University of Washington] At: 18:07 13 March 2008

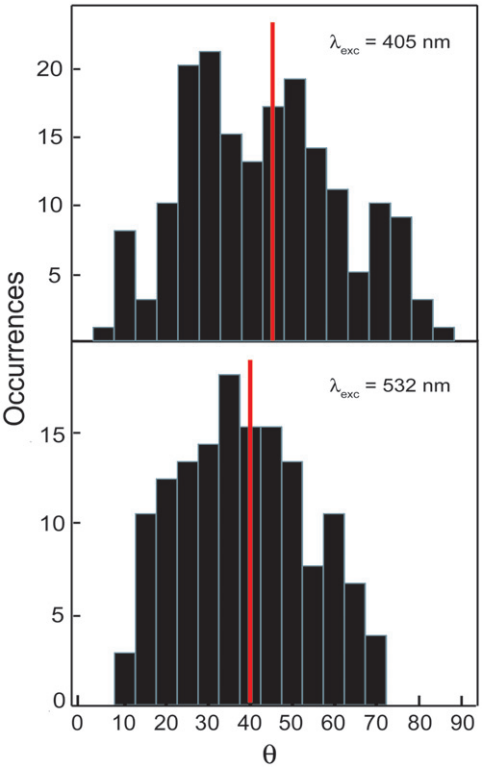

Figure 6. Single-molecule orientational histograms for DCF in KAP. (a) Distribution containing 180 DCF molecules employing 405-nm excitation, with an average value of $42.6 \pm 18.3^{\circ}$ from [100]. (b) Orientations of 151 DCF molecules excited at 532 nm, the average orientation was found to be $38.6 \pm 15.5^{\circ}$ from [100].

The single-molecule orientations of the blue-shifted species were measured using 405-nm excitation to give an average orientation of $20.6 \pm 9.1^{\circ}$ relative to [100] with values ranging from 3.3° to 46.1° for 74 molecules. The single-molecule orientational distributions of KAP/DCM obtained using 488-nm and 405-nm excitation, are overlaid in Figure 7. The averages of the distributions are in good agreement with the ensemble-averaged values and demonstrate the dichroism in KAP/DCM is indeed dependent upon excitation energy. Furthermore, the observed fluorescence time traces from some single molecules (an example is presented in Figure 8) indicate that dual emission is exhibited from DCM in the crystal host. The observation of dual emission verifies that chromophores are incorporated into the host matrix in a distribution of molecular geometries with distinct energies.

Ensemble-averaged polarization spectroscopy of KAP dyed with a variety of luminophores suggests that dyes are oriented during crystal growth. However, by applying single-molecule techniques to these mixed crystals, we discovered that the orientational distributions are wide. Rhodamine derivatives like VR and DCF exist in a wide variety of orientations in KAP, despite the observation of both inter- and intra-sectoral zoning in heavily-dyed crystals. Crystals of KAP/DCM exhibited narrower

Downloaded By: [University of Washington] At: 18:07 13 March 2008

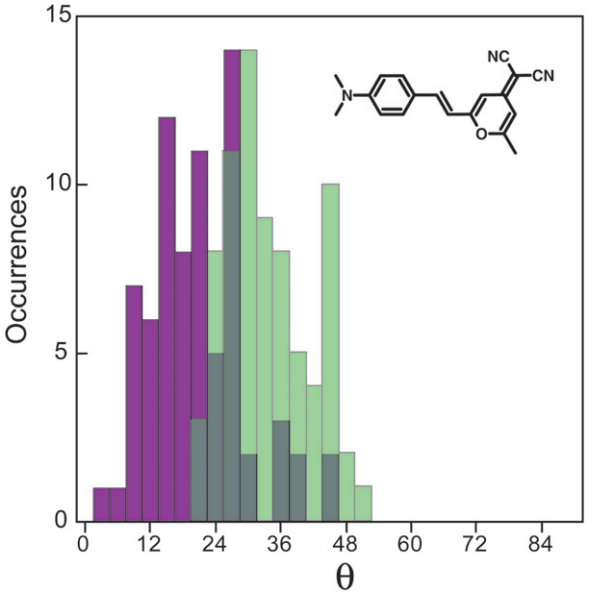

Figure 7. Single-molecule orientational histograms for DCM in KAP employing (purple) 405-nm excitation of 74 molecules, and (green) 488-nm excitation of 75 molecules. The average orientations were determined to be excitation-wavelength dependent, corresponding to $20.6 \pm 9.1^{\circ}$ and $33.6 \pm 7.8^{\circ}$ from,[100] respectively.

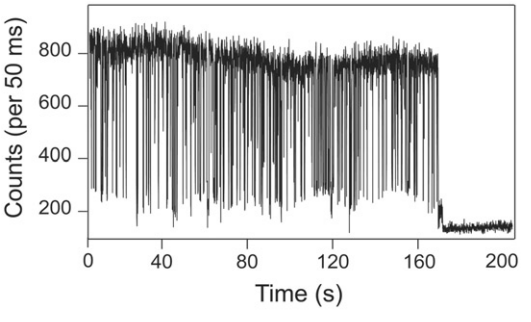

Figure 8. Single-molecule emission intensity over time for an individual molecule of DCM in KAP recorded over 200s employing a 50-ms time bin. The existence of two emissive intensities (~800 and ~200 counts per 50 ms) supports the hypothesis that the molecule exhibits dual emission.

orientational distributions relative to the rhodamine-type chromophores, but demonstrated energy-dependent orientational distributions. Overall, the orientational distributions observed in dyed KAP crystals are indicative of a significant amount of environmental heterogeneity within the KAP lattice.

3. Single-molecule photophysics in dyed composite materials

A common method used to measure molecular photophysics is analysis of the time-dependence of single-molecule emission. Specifically, a single molecule is subjected to

Downloaded By: [University of Washington] At: 18:07 13 March 2008

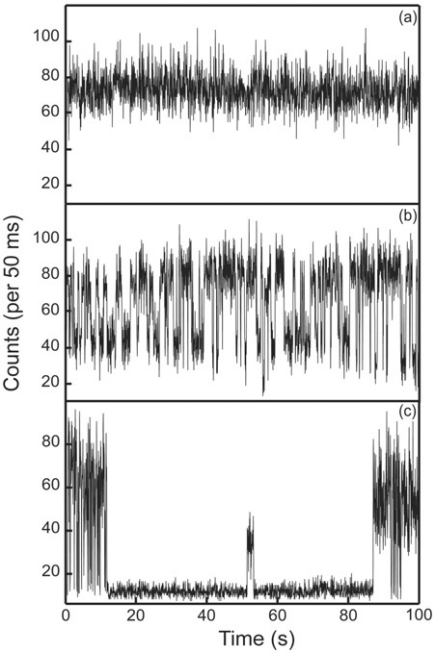

Figure 9. Emission traces (100-s length and 50-ms integration time) of three representative single molecules of VR incorporated in KAP exhibiting (a) persistent emission, (b) periodic blinking, and (c) both fast and slow blinking (i.e. two off events lasting >30 s).

continuous photoexcitation and the variation of the emission with time is measured. A common signature of single-molecule behaviour is the observation of emission intermedience, or 'blinking', as illustrated in Figure 9b. Here, the emission trace of a single rhodamine derivative subjected to continuous irradiation at 532 nm is presented. The trace is characterized by periods of emissive behaviour ('on-times') interdispersed with periods of non-emissive behaviour ('off-times'). Of particular interest is the identification of the non-emissive state and its population and depopulation kinetics, which can be revealed by computing the autocorrelation of the emission intensity or by compiling the distribution of on- and off-times [46,94]. In particular, the histograms of on- and off-times can be described by exponential functions reflecting the rate of intersystem crossing and the decay rate of the triplet state, respectively [95,96] for systems where population and depopulation of the triplet state is responsible for fluorescence intermittency [13,14,94,96–98].

However, many other systems demonstrate more complex blinking behaviour that is not readily assigned to the population and depopulation of an optically dark state with well-defined rate constants. For example, the blinking statistics of single semiconductor nanocrystals are not well described by single-exponential kinetics [99–110]. Figure 10 presents the time-dependent fluorescence intensity observed from a single CdTe quantum dot, and the corresponding on- and off-time histograms that are not well described by a single exponential function indicating that the dark-state population and depopulation kinetics are complex [107]. In fact, the distributions demonstrate power-law behaviour of

Downloaded By: [University of Washington] At: 18:07 13 March 2008

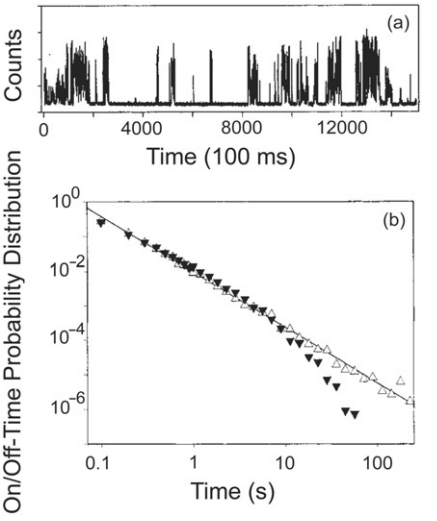

Figure 10. Quantum dot blinking dynamics. (top) Emission from an individual CdTe quantum dot over time. (bottom) The probability distributions for on-times (filled triangles) and off-times (open triangles) are fitted by power laws with exponents of ~1.6. Reproduced with permission from[107].

the form $P_{\text{on/off}} \propto t^{-m}$ where m is referred to as the power-law exponent. Modeling studies have demonstrated that the observation of power-law behaviour is consistent with distributed kinetics involving non-emissive states where the population/depopulation rate constants are not well described by a single value, but instead vary with time [105]. Values for m of roughly 1.5 have been observed for several quantum dot systems, with theoretical treatments suggesting that this value reflects the formation of a non-emissive charged quantum dot through electron transfer [103,105,108,111,112]. However, power-law behaviour in semiconductor quantum dots has been observed to exhibit power-law exponents ranging from 1 to 2, photoinduced modifications to the distributions, as well as insensitivity of excitation power to blinking behaviour. An alternative explanation for power-law behaviour in semiconductor quantum dots is spectral diffusion [101,113–116]. Research continues to establish the nature of the quantum-dot dark state, and the mechanism of its formation.

In comparison to the quantum dot systems, the observation of distributed kinetics in molecular systems is less understood. Typically, the observation of single-molecule blinking has been taken as evidence for molecules undergoing excursions to the triplet state [13,14,94,96–98]. For example, the distribution of delays between consecutive photons from single pentacene molecules in *p*-terphenyl crystals was found to be exponential, consistent with depopulation of the triplet manifold by non-radiative relaxation [97]. The off-time histograms for $DiIC_{18}$ molecules in PMMA and polystyrene were fit by single exponentials, with time constants consistent with the triplet lifetime of the molecule [96]. Conversely, many other studies have observed broad distributions of on- and off-times that are inconsistent with single-exponential rate processes for dark-state population and decay [94,117–127]. Etiologies proposed for distributed kinetics in organic chromophores have included molecular rotation [117],

Downloaded By: [University of Washington] At: 18:07 13 March 2008

conformational flexibility [46,119,121,124], spectral diffusion [11,91,128–130], reversible photooxidation [131,132], and intermolecular electron transfer [118,120,123,125–127]. For example, power-law blinking behaviour of single molecules of rhodamine 6G on glass [123] and in poly(vinyl alcohol) [126] perylene diimide molecules in PMMA [127], as well as the dye Atto565 on glass [125] have been attributed to the formation of non-emissive radicals through electron transfer between the emitter and the surroundings. It is thought that the dynamic environmental heterogeneity characterizing these systems provides for a distribution of electron-transfer rates. Although there is general agreement that blinking is an intrinsic characteristic of single-molecule emission, ambiguity persists regarding the nature of the dark state and the mechanism of dark-state population and depopulation for systems that demonstrate distributed kinetics.

Numerous mechanisms for distributed blinking kinetics have been explored; however, interpretation of these studies is complicated by the heterogeneity of the surrounding environment. Previous studies used crystalline films as surfaces to study molecular photophysics [110], but recognized the further need for studies of chromophores embedded in crystalline materials. We used simple crystals as hosts of complex luminophores to study single-molecule photophysics in well-defined environments [91]. A single crystal matrix is ordered and restrictive with respect to translation and rotation of guest molecules. In addition, molecular bleaching due to photo-oxidation is reduced relative to oxygen-permeable matrices, and the decrease in non-radiative relaxation caused by the restrictive environment both afford enhanced photostability [65]. Dyed crystals are the optimal system for investigating single-molecule photophysics; in particular, determining the nature of the non-emissive state, its population and depopulations kinetics, as well as the coupling of the dark state to photodecomposition pathways.

3.1. *Single-molecule photophysics in dyed salt crystals*

Single-molecule microscopy was used to measure the photophysics of single molecules incorporated into single crystals of KAP [91]. Figure 9 presents emission traces of three representative VR molecules. The molecule in Figure 9a demonstrates persistent emission for the duration of the experiment. In contrast, the molecule in Figure 9b exhibits frequent transitions between on and off states reminiscent of the blinking demonstrated by other molecular fluorophores and semiconductor quantum dots. The emission trace shown in Figure 9c demonstrates substantially different blinking timescales and two off events that last for more than thirty seconds. Similar behaviour was reported for multi-chromophoric dendrimers dispersed in a polymer, where frequent blinking was observed with off events on the order of microseconds accompanied by infrequent off events that lasted hundreds of milliseconds [133]. Although the duration of the two off events in Figure 9c are much longer than typical triplet lifetimes [134], triplet lifetimes of luminophores in mixed crystals can be significantly enhanced relative to solution due to conformational restrictions provided by the host, and phosphorescence lifetimes on the order of seconds to minutes have been observed [68,135].

The blinking dynamics of VR in KAP were measured and quantified in terms of switching rates (s^{-1}), and on- and off-time probability densities. The distribution of switching rates for 205 VR molecules is presented in Figure 11a. The average switching rate was $1.37 \pm 1.94\,s^{-1}$, with the error representing one standard deviation from the mean.

Downloaded By: [University of Washington] At: 18:07 13 March 2008

Of 205 molecules, 79 (38.5%) exhibit persistent emission and are subsequently characterized as simply being 'on'. For the remaining 126 molecules that demonstrate blinking, the distribution of switching rates (Figure 11a, inset) is substantial, ranging from 0.05 to 8.38 s^{-1}. Best fit of this subset of the total distribution to a bi-exponential function corresponds to $A_1 = 480$, $\tau_1 = 0.19$ s and $A_2 = 4.4$, $\tau_2 = 3.4$ s. In summary, these data suggest the presence of two subpopulations in the crystal, molecules that exhibit continual luminescence and the remainder that display a broad distribution of blinking timescales.

What is the origin of the wide variation in photophysical behaviour evident in Figure 11a? To address this question, we examined the connection between the orientational and photophysical heterogeneity demonstrated by KAP/VR. Statistically-improbable molecular orientations (i.e. values beyond one standard deviation from the mean) presumably originate from kinetic rather than thermodynamic factors governing crystal growth, and the photophysical behaviour arising from a kinetically-determined distribution of molecular orientations may differ significantly from the stereochemically most probable docking site. The relationship between photophysics and alignment was investigated by successive measurements of the emission and orientation of

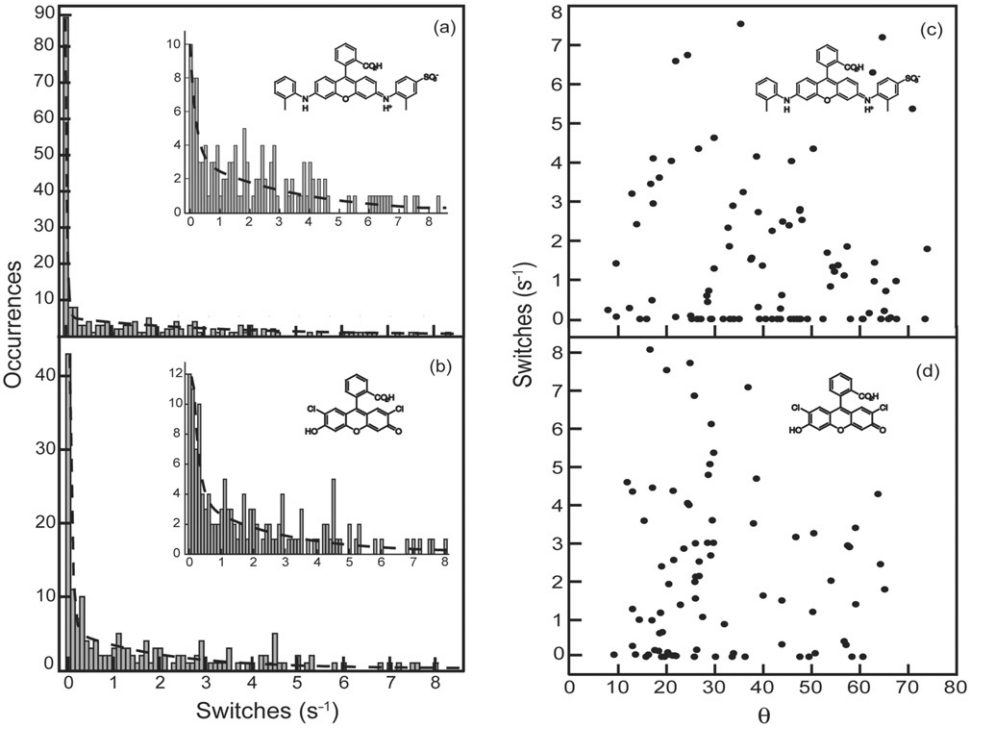

Figure 11. Distribution of switching rates (s^{-1}) for (a) 205 molecules in KAP/VR and (b) 168 molecules in KAP/DCF. The average switching rates were found to be $1.37 \pm 1.94\ s^{-1}$ and $1.64 \pm 1.96\ s^{-1}$, respectively. For KAP/VR, ~40% of the molecules are 'on' (i.e. switching rate = 0 s^{-1}), and the remainder (inset, a) demonstrate a wide variety of switching rates, corresponding to a bi-exponential fit (dashed line). For KAP/DCF, ~20% of the molecules are 'on' and the rest (inset, b) demonstrate bi-exponentially distributed switching rates. (c) Scatter plots of the switching rates (s^{-1}) and orientations of 93 molecules in KAP/VR and (d) 82 molecules in KAP/DCF. No correlation between photophysics and alignment is observed.

Downloaded By: [University of Washington] At: 18:07 13 March 2008

93 molecules in KAP/VR. Plots of the switching rate with respect to orientation are shown in Figure 11c, where no correlation between orientation and photophysical behaviour is evident.

To further characterize the blinking dynamics of single molecules in KAP/VR, the temporal duration of emissive and non-emissive events were compiled into on- and off-time histograms. Figure 12a demonstrates that on-times observed from 40 single molecules range from 0.05 s (the experimental resolution) to 98.8 s. The corresponding off-time distribution consists of events ranging from 0.05 s to 76.0 s (Figure 12b). Both the on- and off-time distributions are peaked at short times, with the number of extremely long events (>30 s) being limited. Consistent with previous analyses, continuous distributions of the on- and off-time probability densities ($P(\tau_{on/off})$) were derived from these data by dividing each value in the on- (off-) time distribution by the average time to its non-zero nearest neighbours. Both $P(\tau_{on})$ and $P(\tau_{off})$ are well described employing a power-law expression of the form $P(\tau_{on/off}) = P_0\tau_{on/off}^{-m_{on/off}}$ and $m_{on/off}$ is the power-law exponent. Plots of $P(\tau_{on})$ and $P(\tau_{off})$ and the best fits to the power-law function corresponding to $P_0(\text{on}) = 371$, $m_{on} = 2.0$, and $P_0(\text{off}) = 208$, $m_{off} = 1.8$ are presented in Figures 12c and 12d, respectively. For comparison, typical power-law exponents observed for other systems are $m \sim 1.7$ for semiconductor nanocrystals [104,108,110,111], $m \sim 2$ for single molecules on glass [123,125], and $m \sim 1.5$ for molecules dispersed in polymers [118,120,136], although most systems demonstrate considerable variability in the power-law exponent. The expectation value for the average time in the on

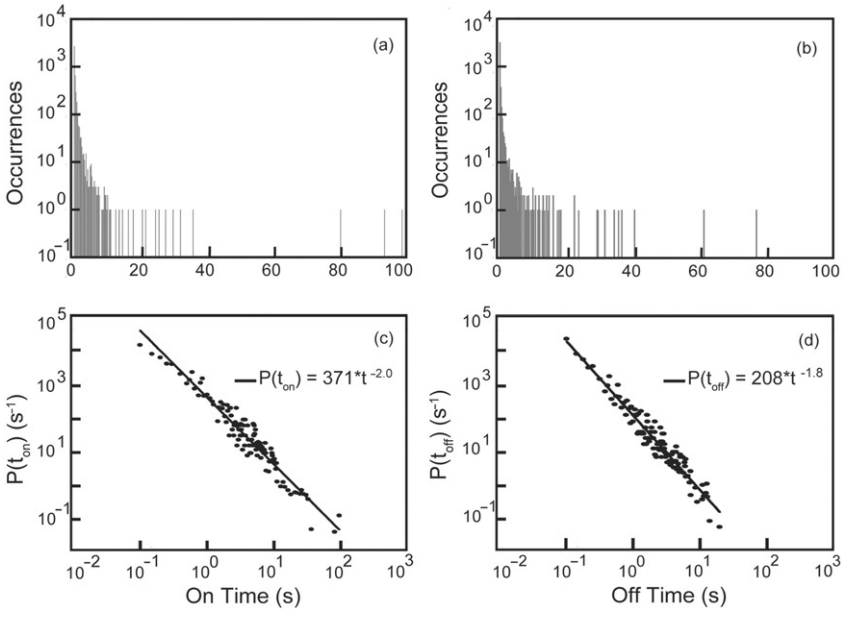

Figure 12. Distribution of on- and off-times for 40 single molecules in KAP/VR. (a) On-time distribution comprised of 4269 emissive events that range from 0.05 to 98.8 s. (b) Off-time distribution containing 4271 non-emissive events ranged from 0.05 to 76.0 s. (c) $P(\tau_{on})$ presented on a logarithmic scale, with a power-law fit to the data (solid line) corresponding to $m_{on} = 2.0$. (d) Corresponding $P(\tau_{off})$ with a power-law fit (solid line) corresponding to $m_{off} = 1.8$.

Downloaded By: [University of Washington] At: 18:07 13 March 2008

or off state ($\langle\tau_{on/off}\rangle$) was obtained from the best fit to the power-law distribution [104,105]. From the power-law fits for KAP/VR, values of $\langle\tau_{on}\rangle = 0.38$ s and $\langle\tau_{off}\rangle = 0.74$ s were obtained. Emission traces for 24 molecules obtained using a 10-ms bin time were compiled to give >10,000 emissive and non-emissive events yielding power-law fits corresponding to $m_{on} = 2.3$, $m_{off} = 2.0$, $\langle\tau_{on}\rangle = 0.03$ s, and $\langle\tau_{off}\rangle = 0.10$ s, demonstrating the dependence of the average on- and off-times on the experimental integration time as well as the insensitivity of m to this perturbation.

3.2. *Power-law blinking behaviour in individual molecules*

Power-law behaviour from individual perylene trimers on glass and in PMMA has been observed [127], consistent with the behaviour determined through the analysis of blinking statistics for collections of these molecules. Since the power-law behaviour observed for the collection of molecules in KAP/VR shown in Figures 12c and 12d could arise from the averaging over many molecules with distributed single-exponential blinking rates, it is important to establish that individual chromophores also demonstrate power-law blinking behaviour. Towards this end, $P(\tau_{on})$ and $P(\tau_{off})$ were calculated for *individual molecules* monitored for one hour, with the observation of emission for the duration of these long-time measurements highlighting the stability that is provided by incorporation into the KAP lattice. All molecules that exhibited blinking for >1000 s (long enough to provide sufficient statistics) produced power-law distributions, with $\langle m_{on}\rangle = 1.8 \pm 0.4$ and $\langle m_{off}\rangle = 1.4 \pm 0.2$. Figure 13 presents the probability distributions for a representative molecule in KAP/VR monitored for one hour, yielding 1645 emissive and 1270 non-emissive events. On- and off-times ranged from the resolution limit (0.05 s) to 169.2 s and 322.2 s, respectively. The distributions for this molecule demonstrated power-law dependence with $P_0(\text{on}) = 88$, $m_{on} = 1.6$, $\langle\tau_{on}\rangle = 1.7$ s, and $P_0(\text{off}) = 44$, $m_{off} = 1.4$, and $\langle\tau_{off}\rangle = 8.3$ s.

Recently, a maximum likelihood estimator (MLE) method for analyzing power-law distributed data with particular application to limited datasets (i.e. individual emitters) has been described [137]. Applying the MLE method to the total dataset consisting of 40 molecules of KAP/VR resulted in power-law exponents of $m_{on} = 1.8$ and $m_{off} = 2.2$. For the molecule in Figure 13, the MLE method produced values of $m_{on} = 2.5$ and $m_{off} = 2.3$, indicating that the power-law exponents for the molecule are closer to the values obtained from analysis of the composite blinking statistics. Overall, these results demonstrate that power-law dependence of blinking dynamics is observed for individual molecules, suggesting that the power-law distribution for the collection of 40 molecules does not arise from averaging of dispersive single-exponential rates for individual molecules (i.e. static), but rather, reflects dynamically-changing rate constants for dark-state population and depopulation.

3.3. *Distributed kinetics models*

Previous authors have used Monte Carlo (MC) simulations based on an electron-tunnelling model to reproduce the distributed kinetics observed in blinking studies of semiconductor quantum dots and for molecular fluorophores [105,125]. We performed

Downloaded By: [University of Washington] At: 18:07 13 March 2008

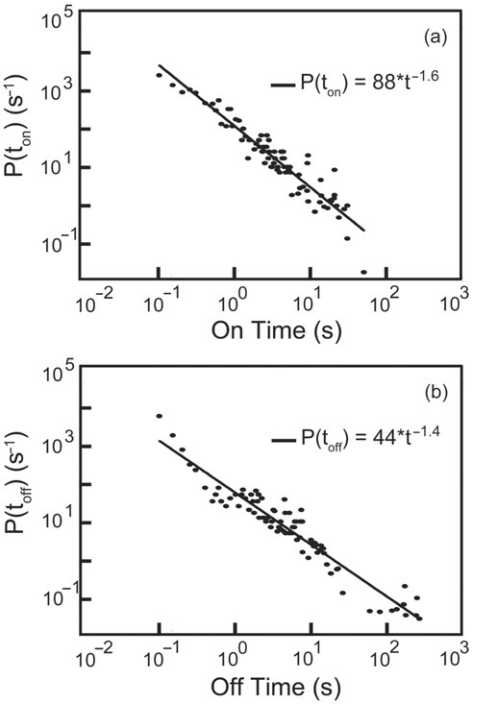

Figure 13. Logarithmic plots of the probability distributions of on-time (a) and off-times (b) for an *individual molecule* in KAP/VR, with power-law fits (solid lines) corresponding to $m_{on} = 1.6$ (least-squares fitting), 2.5 (MLE) and $m_{off} = 1.4$ (least-squares fitting), 2.3 (MLE).

MC simulations described in detail elsewhere [91] of blinking dynamics employing a model with three electronic levels: the singlet ground state ($|1\rangle$), the singlet excited state ($|2\rangle$), and a 'dark' state ($|3\rangle$) (Figure 14a). The photoexcitation rate constant (k_{12}) is restricted to be $1 \times 10^6\,s^{-1}$ based on the experimental laser power and absorption cross section of VR. The radiative rate constant (k_{21}) is fixed at $3.7 \times 10^8\,s^{-1}$ consistent with the measured fluorescence lifetime of KAP/VR. To account for power-law behaviour, the dark-state population (k_{23}) and depopulation (k_{31}) rate constants were modeled as follows: $k_{ij} = \kappa_{ij} e^{-x}$. In this expression, i and j are the initial and final states, respectively, κ_{ij} is the pre-exponential factor, and x is a random number generated from an exponential distribution. For both $P(\tau_{on})$ and $P(\tau_{off})$ to follow power-law behaviour, pathways to and from the dark state must be distributed. To model blinking dynamics in KAP/VR, 40 simulations were performed with κ_{23} and κ_{31} set to $10^6\,s^{-1}$ and $10^4\,s^{-1}$, respectively. Figure 14b presents a simulated 100-s emission trace employing a 50-ms bin time, and the corresponding probability densities determined using a threshold of the average between on and off intensities. The probability distributions of on- and off-times from the simulated data are presented in Figures 14c and 14d, respectively. Best fit corresponded to power-law expressions with $P_0(\text{on}) = 498$, $m_{on} = 2.1$, $\langle\tau_{on}\rangle = 0.30$ and $P_0(\text{off}) = 74$, $m_{off} = 2.0$, $\langle\tau_{off}\rangle = 0.34\,s$, in good agreement with the experimental distributions.

Downloaded By: [University of Washington] At: 18:07 13 March 2008

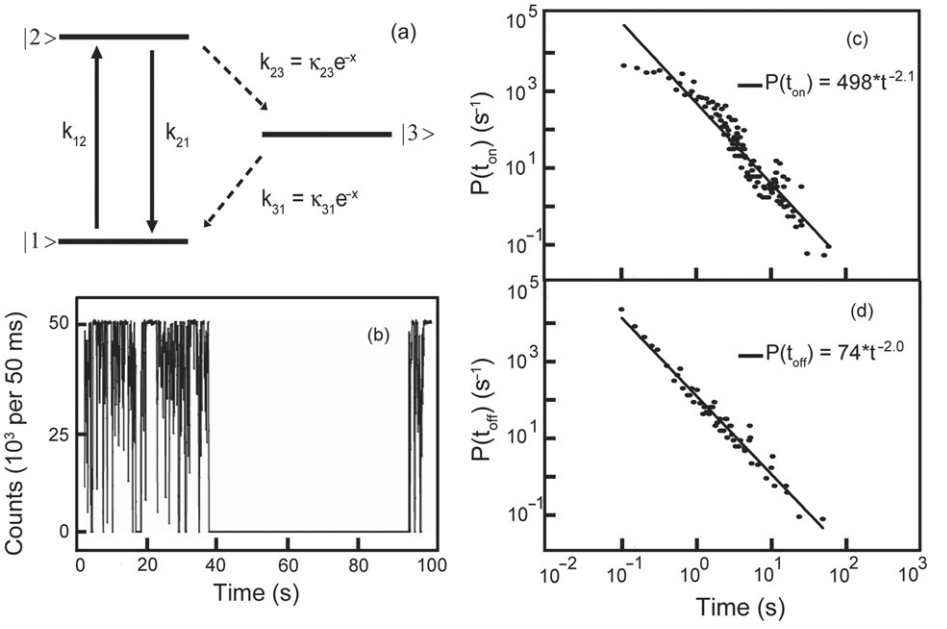

Figure 14. Monte Carlo (MC) Simulations. (a) Physical model employed in the MC simulations. Three electronic levels considered correspond to: the singlet ground state ($|1\rangle$), the singlet excited state ($|2\rangle$), and a 'dark' state ($|3\rangle$). The photoexcitation and emission rate constants are fixed based on experimental conditions (solid arrows), while the dark-state population (k_{23}) and depopulation (k_{31}) rate constants are distributed (dashed arrows). (b) Representative simulated emission trace employing a 50-ms bin, 1-ns computational time step, and $k_{12} = 10^6\,s^{-1}$, $k_{21} = 3.7 \times 10^8\,s^{-1}$, $\kappa_{23} = 10^6\,s^{-1}$, and $\kappa_{31} = 10^4\,s^{-1}$. The resulting on- and off-time probability distributions from 40 simulated traces and corresponding power-law fits are shown in (c) $m_{on} = 2.1$ and (d) $m_{off} = 2.0$, respectively.

3.4. *Role of the environment in power-law behaviour*

To explore the role of environment on blinking dynamics as well as the variation in the microscopic rate constants predicted by the MC simulations, we performed blinking studies of VR in poly(methyl acrylate) (PMA, $T_g = 9°C$). The emission intensity following circularly-polarized excitation was collected on two polarization-sensitive detectors and summed in order to monitor blinking. The emission traces of 16 molecules in PMA/VR under nitrogen at room temperature were used to assemble the on- and off-time probability distributions containing 1519 emissive and 1510 non-emissive events that ranged from 0.05 s to 10.5 s and 39.9 s, respectively. The on- and off-time probability distributions were fit by power laws: $P_0(\text{on}) = 69$, $m_{on} = 2.6$, $\langle\tau_{on}\rangle = 0.12$ s, and $P_0(\text{off}) = 103$, $m_{off} = 2.4$, and $\langle\tau_{off}\rangle = 0.17$ s (Figure 15). Considering the intrinsic error in the power-law exponent in roughly 0.3 [91], m_{on} and m_{off} are statistically equivalent for VR in KAP and PMA. To model the blinking dynamics of VR in PMA, MC simulations were performed with κ_{23} and κ_{31} set to $5 \times 10^7\,s^{-1}$ and $5 \times 10^3\,s^{-1}$, respectively. Best fit corresponded to a power-law expression with $P_0(\text{on}) = 182$, $m_{on} = 2.2$, $\langle\tau_{on}\rangle = 0.20$ and $P_0(\text{off}) = 67$, $m_{off} = 2.0$, $\langle\tau_{off}\rangle = 0.26$ s, in good agreement with the experimental data.

The rate constants for population and depopulation of the non-emissive state predicted by MC simulations are significantly different for VR in KAP relative to PMA. For VR

Downloaded By: [University of Washington] At: 18:07 13 March 2008

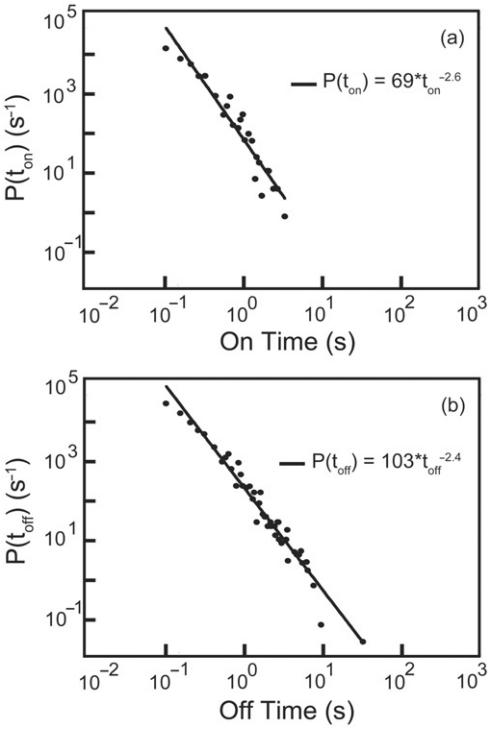

Figure 15. Probability distributions of on- and off-times for 16 molecules of VR in PMA under nitrogen at room temperature. The power-law fits for on- and off-times are shown in (a) $m_{on} = 2.6$ and (b) $m_{off} = 2.4$, respectively.

in the polymer, power-law behaviour was modelled using rate constants to and from the non-emissive state of $5 \times 10^7\,s^{-1}$ and $5 \times 10^3\,s^{-1}$, respectively. In contrast, the blinking dynamics of VR in KAP were modeled with a population rate constant 50 times slower and depopulation twice as fast as the kinetics in PMA. Previous MC simulations of single Atto565 molecules immobilized on glass produced power-law exponents of $m_{on} = 2.8$ and $m_{off} = 2.0$, using κ_{23} and κ_{31} values of $4 \times 10^9\,s^{-1}$ and $10^6\,s^{-1}$ [125]. For MC simulations of quantum-dot blinking, previous authors obtained $m_{on} = 2.2$ and $m_{off} = 2.0$, using κ_{23} and κ_{31} values of $10^7\,s^{-1}$ and $10^5\,s^{-1}$ [105]. Comparison of these results to our experimental and MC simulated data for VR in KAP and PMA demonstrates the relative insensitivity of the power-law exponent to the pre-exponential factors. A substantial difference between the blinking dynamics of VR in KAP and PMA was not observed. However, the role of the dielectric environment on power-law behaviour has been demonstrated for semiconductor quantum dots embedded in a series of polymer hosts (e.g. PMMA, PVA) and atop crystalline films (e.g. *p*-terphenyl, NaCl) [110]. More recently, Clifford *et al*. [136] demonstrated that blinking behaviour of the dye Atto647N could be significantly modified by manipulation of the heterogeneity imposed by the surrounding matrix; universal power-law behaviour was observed for molecules in zeonex and PVK, mono- or stretched-exponential behaviour was observed for molecules in PVA and an aqueous environment.

Downloaded By: [University of Washington] At: 18:07 13 March 2008

3.5. *The origin of distributed kinetics in chromophores*

The origin of distributed kinetics in organic chromophores has been a recent topic of interest. Akin to the distributed kinetics model for semiconductor quantum dot blinking, power-law blinking statistics of single molecules is generally attributed to charge separation and recombination mechanisms including: diffusion-controlled charge transfer [112,138], photoinduced spectral diffusion of donor and acceptor levels, [107,112,136] and electron or hole tunnelling [104,105,110,111,127]. The diffusion-controlled electron transfer model (DCET [139,140]) involves charge ejection from the excited state and distributed recombination rates that are a consequence of the disordered surroundings [138]. Although power-law behaviour for the off-times is predicted by DCET, single-exponential statistics are expected for the on-times, consistent with a single rate for charge separation from the excited state. Thus, the DCET model cannot account for universal power-law behaviour (i.e. both on- and off-times being power-law distributed). The photoinduced spectral diffusion model involves one-dimensional diffusion in energy space of donor and acceptor energy levels[101] and predicts power-law exponents of 1.5 [112,141]. However, the results for KAP/VR and PMA/VR ($m \sim 2$) are inconsistent with the predictions of this model; moreover, no excitation power-induced changes to the blinking statistics were observed, an expected upshot of photoinduced processes.

Alternatively, power-law statistics for the on- and off-times for single molecules of rhodamine 6G in poly(vinyl alcohol) [126], and on glass [123], perylene diimide molecules in PMMA [127], as well as Atto565 on glass [125] have been assigned to the formation of non-emissive radicals by electron tunnelling with power-law exponents ranging between 1 and 2. In these systems, the dynamic and heterogeneous environment that surrounds the molecule is thought to be responsible for an exponential distance-dependence of tunnelling rates [105]. Support for this hypothesis was provided by Zondervan *et al.*, who measured a weak temperature dependence of the lifetime of the dark state consistent with electron tunnelling, as well as the ESR spectrum of a photoexcited polymer film containing single molecules of rhodamine 6G, and observed a transition consistent with radical formation [126].

In contrast to the aforementioned studies, we observed distributed kinetics for molecules incorporated in a rigid, ordered, and well-defined crystalline environment. This observation is both informative and confounding with respect to the electron transfer model that relies on the disordered nature of the surrounding matrix to explain the origin of the distributed kinetics. Furthermore, if charge transfer were occurring in the crystal, one would expect a correlation between molecular orientation and blinking dynamics consistent with the orientational- and distance-dependence of electron transfer. However, no correlation between molecular orientation and blinking was observed (Figure 11c). Moreover, power-law exponents of roughly 2 are inconsistent with the proposed electron transfer models. Given the issues surrounding assignment of the distributed kinetics for KAP/VR to intermolecular electron transfer, other origins for power-law dependence of the blinking dynamics were explored.

Extended dark periods in single-molecule emission studies have also been attributed to time- and environment-dependent conformational changes of molecules such as the formation of twisted intramolecular charge transfer (TICT) conformer [46]. In the case of VR, it is possible that variation in blinking behaviour reflects a distribution of

Downloaded By: [University of Washington] At: 18:07 13 March 2008

conformational flexibility provided by various crystal nano-environments. To explore this hypothesis, linear-response time-dependent Hartree–Fock calculations (TD-HF[142]) were performed to determine the conformational dependence of the excited-state properties of VR. Computations provided evidence that more than one molecular conformation is accessible at room temperature, and conformationally-induced spectral diffusion may lead to the variation in blinking behaviour. Yet, the ground-state potential energy surface of VR demonstrated that the dark conformers exist in relatively shallow minima (~2 kcal/mol).

To further explore the role of conformational flexibility in the distributed kinetics of VR, we performed blinking experiments on KAP/DCF (Figure 4). DCF lacks the sulfonated aryl ring such that this potential source for conformational dependence of the transition dipole moment is eliminated. The distribution of switching rates observed for KAP/DCF (Figure 11b) is remarkably similar to that observed for KAP/VR (Figure 11a), and again suggested the existence of two photophysical subpopulations in the crystal. Moreover, no obvious correlation between absorption dipole moment orientation and blinking dynamics was observed (Figure 11d), reminiscent of the case for KAP/VR. On- and off-time histograms were compiled from the emission time traces of 72 single molecules of DCF. Figure 16 demonstrates that power-law behaviour is observed for KAP/DCF, with best fit to the power-law expression corresponding to $P_0(\text{on}) = 308$, $m_{\text{on}} = 1.9$, $\langle\tau_{\text{on}}\rangle = 0.44$ and $P_0(\text{off}) = 284$, $m_{\text{off}} = 1.7$, $\langle\tau_{\text{off}}\rangle = 0.76$ s. Overall, our results demonstrate that power-law behaviour is observed for single molecules in both KAP/DCF

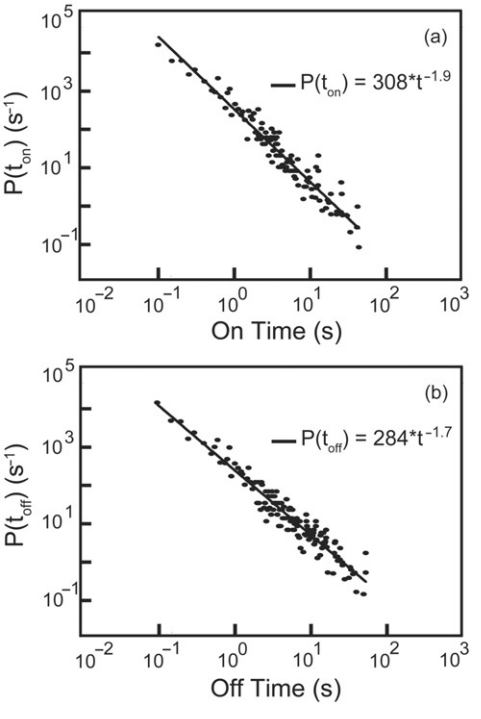

Figure 16. Probability distributions of on-times (a) and off-times (b) for 72 molecules in KAP/DCF, with power-law fits (solid lines) corresponding to $m_{\text{on}} = 1.9$ and $m_{\text{off}} = 1.7$, respectively.

Downloaded By: [University of Washington] At: 18:07 13 March 2008

and KAP/VR, and this similarity suggests that the distributed kinetics for KAP/VR are not associated with conformational flexibility.

Relative to glass surfaces and polymer films, the KAP lattice provides a uniquely well-defined and ordered environment. However, the broad orientational distributions of VR and DCF in KAP provided evidence that the first-coordination spheres of embedded dyes are surprisingly diverse, despite the specific chemical zoning that is observed in heavily-dyed crystals. This environmental heterogeneity, as well as time-dependent relaxation of the molecule with respect to the surrounding dielectric, is proposed as the origin of the distributed kinetics observed in KAP. Preliminary TD-DFT calculations on the anionic form of VR, the principal species in the crystal-growth solution, predict that the visible absorption is hypsochromically shifted up to 100 nm for when a potassium cation was introduced near its sulfonate or carboxylate moiety [142]. Since distributed kinetics were observed for an individual molecule, a dynamically-changing property must be responsible for blinking behaviour. Accordingly, two possible mechanisms for distributed kinetics are proposed: (1) time-dependent geometrical changes in the first-coordination sphere of a fixed molecule (i.e. dynamical spectral diffusion) and (2) dynamic environmental and/or conformational heterogeneity in combination with a charge separation and recombination mechanism that occurs via exponentially-varying population and depopulation rates. Both spontaneous [11,13] and photoinduced [143] spectral diffusion have been observed for single molecules in mixed crystals. Single pentacene molecules that exhibited spectral diffusion were attributed to crystal sites with local disorder such that the local strain or dielectric environment is far from equilibrium [11,13,144].

3.6. *Memory in single-molecule emission*

To gain more insight into the origin of distributed kinetics in quantum dots, previous studies examined the correlations between adjacent on- and off-times [102,104,109]. The idea behind these studies is that the presence or absence of correlations provides information on the timescale for dielectric fluctuations affecting the value of k_{ij}. If the rate constants governing the population and depopulation of the dark state vary slower than the blinking rate, then adjacent emissive and non-emissive events should be correlated (i.e. memory). Conversely, if the fluctuations are fast compared to the blinking rate, the temporal duration of adjacent emissive/non-emissive events will not be correlated. Stefani *et al*. [109] demonstrated that memory is indeed observed for ZnCdSe quantum dots, suggesting that the fluctuations occur more slowly than the timescale for blinking. In contrast, studies by Nesbitt and coworkers [102,104] found no correlation in the emission from InP and CdSe quantum dots, but power-law behaviour was still observed. This observation suggests that k_{ij} fluctuations occur on the blinking timescale, consistent with charge ejection changing the local environment thereby erasing any memory between successive blinking events. The relationship between power-law behaviour and the presence (or absence) of memory effects in the blinking dynamics of semiconductor quantum dots has yet to be definitively established.

We recently examined memory effects in the blinking dynamics of VR in KAP [145]. That memory has not been previously reported for molecular systems is likely due to the advent of photobleaching that limits the statistics that can be acquired on a single molecule. However, when incorporated into KAP, single fluorophores can exhibit

Downloaded By: [University of Washington] At: 18:07 13 March 2008

emission for thousands of seconds. With this advantage, we are able to study the blinking dynamics of VR over a time range that provides a sufficient statistical sample of emissive/non-emissive events allowing for the observation of memory. Correlations between adjacent on- and off-times were examined by analyzing *xy*-plots on logarithmic scales consistent with previous studies [109]. First, the blinking dynamics of 40 molecules in KAP/VR were compiled to produce plots of the temporal durations of successive emissive and non-emissive events as shown in Figure 17a. The linear Pearson correlation coefficient ($R_{\log}$) was used to quantify correlations between adjacent times. The limiting values of $R_{\log}$ are 1 and -1 corresponding to positive and negative correlation, respectively, and $R_{\log}$ values close to zero indicate no correlation. Therefore, deviations from zero suggest correlations, and are visually manifested as an enhancement of point density along the diagonal ($x = y$). The greater point density along the diagonal for plots of consecutive on-times (Figure 17a) and off-times (Figure 17b) demonstrates the existence of memory for VR in KAP. Consistent with this observation, adjacent on-times and adjacent off-times exhibit positive correlations with $R_{\log}$ values of 0.48 and 0.50, respectively. In contrast, the plot of consecutive on- and off-times (Figure 17c) demonstrates a paucity of points

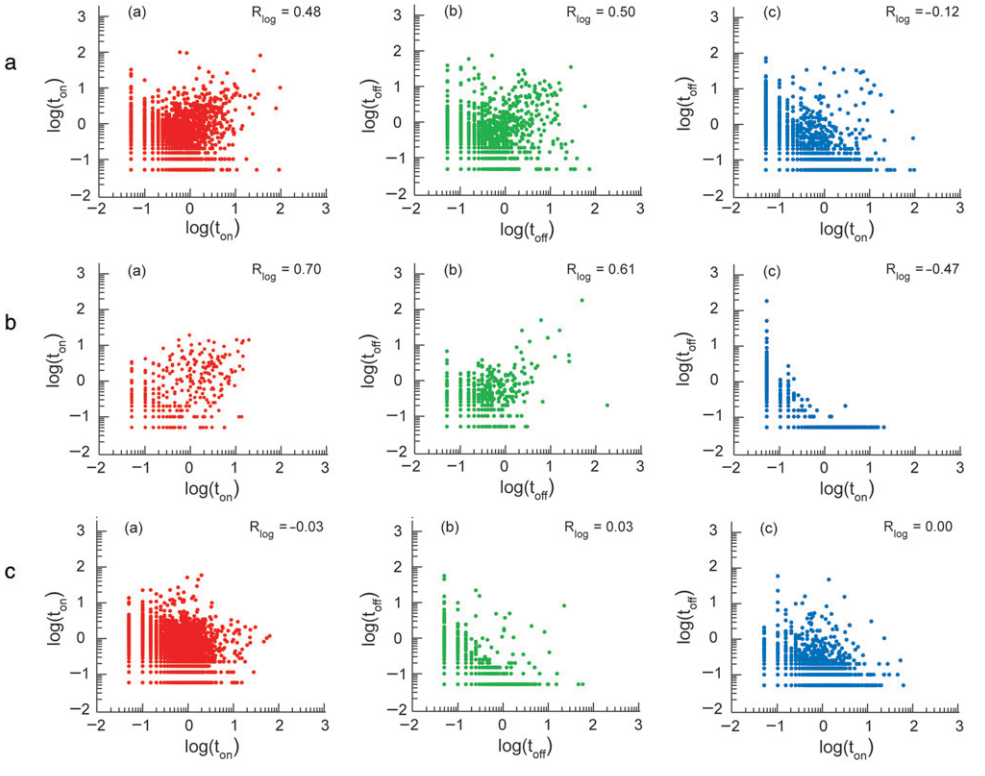

Figure 17. Memory in single-molecule emission. Scatter plots of on-times ($\log(t_{on})$ vs. $\log(t_{on})$), off-times ($\log(t_{off})$ vs. $\log(t_{off})$), and on- and off-times ($\log(t_{on})$ vs. $\log(t_{off})$) are presented on logarithmic scales with corresponding correlation coefficients ($R_{\log}$). a. Correlations of adjacent on- and off-times (in seconds) obtained from 40 molecules of VR in KAP. b. Correlations from an individual molecule in KAP/VR. c. Correlations obtained from 40 Monte Carlo simulated emission traces demonstrating the absence of memory.

Downloaded By: [University of Washington] At: 18:07 13 March 2008

along the diagonal, consistent with anticorrelation of successive on and off events. Quantitatively, consecutive on- and off-times exhibit a weak negative correlation ($R_{\log} = -0.12$) consistent with anticorrelation.

In order to establish that individual molecules exhibit memory, and that the correlations evident in Figure 17a do not arise from sampling over many populations, we performed a similar correlation analysis on the emission observed from individual molecules. All molecules that exhibited blinking for > 1000 s (long enough to provide sufficient statistics) produced power-law behaviour and non-zero correlation coefficients, with $\langle R_{\log,\mathrm{on}} \rangle = 0.26 \pm 0.23$, $\langle R_{\log,\mathrm{off}} \rangle = 0.45 \pm 0.24$, and $\langle R_{\log,\mathrm{onoff}} \rangle = -0.21 \pm 0.18$, consistent with the coefficients observed for the collection of molecules. Representative correlation plots of adjacent on- and off-times for a single molecule of KAP/VR are presented in Figure 17b. In agreement with the ensemble correlations, the molecule exhibits positive correlations for consecutive on-times ($R_{\log} = 0.70$) and consecutive off-times ($R_{\log} = 0.61$) as well as anticorrelated on- and off-times ($R_{\log} = -0.47$).

In order to ensure that the observed memory effects are not artifacts of threshold selection or data analysis, we performed Monte Carlo simulations employing our previously described distributed kinetics model, subjected the simulated emission data to the analysis presented above, and investigated the resulting on- and off-time correlations. The stochastic nature of the simulations should render the resulting blinking dynamics memoryless. Figure 17c presents scatter plots of adjacent on- and off-times from 40 Monte Carlo simulations of KAP/VR blinking dynamics. Indeed, no correlations are evident in the plots and the correlation coefficients are very close to zero. These results validate that the memory effect observed for VR in KAP do not result from threshold selection or the data analysis employed.

What can be learned from the observation of memory in KAP/VR? Primarily, this study demonstrated that the blinking dynamics of single molecules can be correlated. Memory between consecutive on- and off-times in the emission of single VR molecules in KAP indicates that the timescale for fluctuations in the population and depopulation kinetics of the non-emissive state are slower than the typical blinking rate. The average blinking rate for KAP/VR was found to be $1.37 \pm 1.94\,\mathrm{s}^{-1}$; therefore, fluctuations in k_{ij} must occur on a relatively slower timescale. The correlations also provide information about the nature of the dark state. One hypothesis for distributed kinetics in KAP/VR is based on time-dependent changes in the configuration of VR relative to its local environment leading to spectral diffusion. The observation of an anticorrelation between consecutive on- and off-times is consistent with this hypothesis, since the state energies are thought to fluctuate in concert with changing guest–host interactions. That is, when the non-emissive state is closer in energy to the ground state relative to the first excited state, the non-emissive state will be populated slowly (small k_{ij}) and then decay rapidly to the ground state (large k_{ij}). Therefore, the observation of anticorrelation of adjacent on and off events directly supports the spectral diffusion hypothesis.

The observation of memory in the emission from single molecules in KAP/VR supports the hypothesis that spectral diffusion is responsible for power-law distributed blinking in this system. To further explore the role of spectral diffusion for KAP/VR as well as dye-doped polymer films, measurements of single-molecule emission energy over time will be performed. Furthermore, if configurational changes between guest and host lead to spectral diffusion, temperature-dependent blinking studies should reveal changes to the

Downloaded By: [University of Washington] At: 18:07 13 March 2008

distributions of on- and off-times as well as the correlations between adjacent blinking events as the temperature is decreased and motions are restricted. We previously demonstrated that VR exhibits a broad orientational distribution in KAP, suggesting a significant amount of environmental heterogeneity in the dyed crystal. Consequently, blinking studies on dyed crystals that exhibit narrow orientational distributions (i.e. basic pyranine in K_2SO_4 [66]) where environmental heterogeneity is minimized will be performed.

4. Summary

Here we have reviewed the literature involving single-molecule studies of dyed-composite materials, work motivated by salient issues in materials chemistry. In particular, the current understanding of physical phenomena such as the establishment of molecular order and complex molecular photophysics in condensed environments was described. Consistent with essentially all single-molecule studies, the information gained was simply not possible through measurement of the ensemble. Still, there are many questions that remain to be explored. For instance, what governs the breadth of the orientational distributions observed in mixed crystals? What is the extent to which temperature modifies the reorientational potential created by the polymer environment? In addition, novel approaches by which to establish molecular order are on the horizon. For example, there is much current interest with regards to establishing molecular order in host materials where the molecular reorientational space is of reduced dimension. Single-molecule techniques are capable of directly evaluating and guiding this interesting approach to establishing molecular order in composite materials. The origin of dispersed kinetics for individual chromophores in condensed environments remains unclear. In addition, does there exist a common origin for this behaviour in widely varying materials (e.g. quantum dots versus dyed crystals)? Such issues are interesting from both a fundamental and applied perspective, and it is anticipated that further work in this area will provide dramatic insight into the issue of dispersed kinetics, insight that can only be achieved using single-molecule techniques.

Acknowledgements

The authors thank the National Science Foundation for the generous support of this work through the Center on Materials and Devices for Information Technology Research (DMR-0120967). BK acknowledges NSF grant CHE-0349882.

References

[1] C. Gooijer, F. Ariese, and J.W. Hofstraat, in *Chemical Analysis: A Series of Monographs on Analytical Chemistry and its Applications,* edited by J.D. Winefordner (John Wiley & Sons, New York, 2000), Vol. 156.
[2] D.S. McClure, *Electronic Spectra of Molecules and Ions in Crystals,* (Academic Press, New York, 1959).
[3] E.V. Shpol'skii, A.A. Il'ina, and L.A. Klimova, Dokl. Akad. Nauk SSSR **87**, 935 (1952).
[4] A.A. Gorokhovskii, R.K. Kaarli, and L.A. Rebane, JETP Letters **20**, 216 (1974).
[5] B.M. Kharlamov, L.A. Bykovskaya, and R.I. Personov, Chem. Phys. Lett. **50**, 407 (1977).

Downloaded By: [University of Washington] At: 18:07 13 March 2008

[6] B.M. Kharlamov, R.I. Personov, and L.A. Bykovskaya, Optik. Spektros. **39**, 240 (1975).
[7] R.I. Personov, E.I. Alshits, L.A. Bykovska, and B.M. Kharlamo, Zhurnal Eksperimentalnoi I Teoreticheskoi Fiziki **65**, 1825 (1973).
[8] R.I. Personov, E.I. Alshitz, and L.A. Bykovska, JETP Lett. USSR **15**, 431 (1972).
[9] R. Lange, W. Grill, and W. Martienssen, Europhys. Lett. **6**, 499 (1988).
[10] W.E. Moerner and L. Kador, Phys. Rev. Lett. **62**, 2535 (1989).
[11] W.P. Ambrose, T. Basche, and W.E. Moerner, J. Chem. Phys. **95**, 7150 (1991).
[12] L. Kador, D.E. Horne, and W.E. Moerner, J. Phys. Chem. **94**, 1237 (1990).
[13] M. Orrit and J. Bernard, Phys. Rev. Lett. **65**, 2716 (1990).
[14] T. Basche, S. Kummer, and C. Brauchle, Nature **373**, 132 (1995).
[15] T. Basche, W.E. Moerner, M. Orrit, and H. Talon, Phys. Rev. Lett. **69**, 1516 (1992).
[16] W.E. Moerner, J. Chem. Phys. **117**, 10925 (2002).
[17] W.E. Moerner, R.M. Dickson, and D.J. Norris, *Adv. Atom. Mol. Opt. Phys.* (Academic Press, San Diego, 1998), Vol. 38, p. 193.
[18] W.E. Moerner and D.P. Fromm, Rev. Sci. Instrum. **74**, 3597 (2003).
[19] W.E. Moerner and M. Orrit, Science **283**, 1670 (1999).
[20] P. Tamarat, A. Maali, B. Lounis, and M. Orrit, J. Phys. Chem. A. **104**, 1 (2000).
[21] P.M. Wallace, D.R.B. Sluss, L.R. Dalton, B.H. Robinson, and P.J. Reid, J. Phys. Chem. B. **110**, 75 (2006).
[22] W.E. Moerner, New J. Phys. **6**, 88 (2004).
[23] K.A. Firestone, P. Reid, R. Lawson, S.H. Jang, and L.R. Dalton, Inorg. Chim. Acta. **357**, 3957 (2004).
[24] B.H. Robinson, L.R. Dalton, A.W. Harper, A. Ren, F. Wang, C. Zhang, G. Todorova, M. Lee, R. Aniszfeld, S. Garner, A. Chen, W.H. Steier, *et al.*, Chem. Phys. **245**, 35 (1999).
[25] Y.Q. Shi, C. Zhang, H. Zhang, J.H. Bechtel, L.R. Dalton, B.H. Robinson, and W.H. Steier, Science **288**, 119 (2000).
[26] P.N. Prasad and D.J. Williams, *Introduction to Nonlinear Optical Effects in Molecules and Polymers*. (John Wiley & Sons, New York, 1991).
[27] B.H. Robinson and L.R. Dalton, J. Phys. Chem. A **104**, 4785 (2000).
[28] F. Guttler, M. Croci, A. Renn, and U.P. Wild, Chem. Phys. **211**, 421 (1996).
[29] F. Guttler, J. Sepiol, T. Plakhotnik, A. Mitterdorfer, A. Renn, and U.P. Wild, J. Lumin. **56**, 29 (1993).
[30] M.D. Ediger, Ann. Rev. Phys. Chem. **51**, 99 (2000).
[31] J.A. Teetsov and D.A. Vanden Bout, J. Amer. Chem. Soc. **123**, 3605 (2001).
[32] G. Adam and J.H. Gibbs, J. Chem. Phys. **43**, 139 (1965).
[33] I. Chang and H. Sillescu, J. Phys. Chem. B **101**, 8794 (1997).
[34] D.J. Fox and P.J. Flory, J. Appl. Phys. **21**, 581 (1950).
[35] W. Kauzmann, Chem. Rev. **43**, 219 (1948).
[36] C.Y. Lu and D.A. Vanden Bout, J. Chem. Phys. **125**, 124701 (2006).
[37] A. Dhinojwala, G.K. Wong, and J.M. Torkelson, J. Chem. Phys. **100**, 6046 (1994).
[38] A.P. Bartko, K.W. Xu, and R.M. Dickson, Phys. Rev. Lett. **89**, 026101 (2002).
[39] N. Tomczak, R.A.L. Vallee, E. van Dijk, M. Garcia-Parajo, L. Kuipers, N.F. van Hulst, and G.J. Vancso, Euro. Poly. J. **40**, 1001 (2004).
[40] H. Finkelmann and D. Day, Makromol. Chem. **180**, 2269 (1979).
[41] H. Finkelmann, D. Naegele, and H. Ringsdorf, Makromol. Chem. **180**, 803 (1979).
[42] C.Y.J. Wei, Y.H. Kim, R.K. Darst, P.J. Rossky, and D.A. Vanden Bout, Phys. Rev. Lett. **95**, 173001 (2005).
[43] A. Dhinojwala, G.K. Wong, and J.M. Torkelson, Macromol. **26**, 5943 (1993).
[44] R. Zondervan, F. Kulzer, G.C.G. Berkhout, and M. Orrit, Proc. Nat. Acad. Sci. **104**, 12628 (2007).
[45] K.D. Weston and L.S. Goldner, J. Phys. Chem. B **105**, 3453 (2001).
[46] Y.W. Hou and D.A. Higgins, J. Phys. Chem. B **106**, 10306 (2002).
[47] R.A.L. Vallee, N. Tomczak, G.J. Vancso, L. Kuipers, and N.F. van Hulst, J. Chem. Phys. **122**, 114704, (2005).
[48] K.A. Willets, S.Y. Nishimura, P.J. Schuck, R.J. Twieg, and W.E. Moerner, Acc. Chem. Res. **38**, 549 (2005).
[49] K.D. Singer, J.E. Sohn, and S.J. Lalama, Appl. Phys. Lett. **49**, 248 (1986).
[50] M. Stahelin, C.A. Walsh, D.M. Burland, R.D. Miller, R.J. Twieg, and W. Volksen, J. Appl. Phys. **73**, 8471 (1993).
[51] H.L. Hampsch, J. Yang, G.K. Wong, and J.M. Torkelson, Macromolecules **23**, 3640 (1990).
[52] J. Vydra and M. Eich, Appl. Phys. Lett. **72**, 275 (1998).
[53] V. Le Floc'h, S. Brasselet, J.F. Roch, and J. Zyss, J. Phys. Chem. B **107**, 12403 (2003).
[54] D.R.B. Sluss, P.M. Wallace, K.D. Truong, B.H. Robinson, L.R. Dalton, and P.J. Reid, Proc. SPIE **6331**, 63310K (2006).
[55] R.M. Dickson, D.J. Norris, and W.E. Moerner, Phys. Rev. Lett. **81**, 5322 (1998).
[56] H. Uji-i, S.M. Melnikov, A. Deres, G. Bergamini, F. De Schryver, A. Herrmann, K. Mullen, J. Enderlein, and J. Hofkens, Polymer **47**, 2511 (2006).
[57] J.J. Macklin, J.K. Trautman, T.D. Harris, and L.E. Brus, Science **272**, 255 (1996).

Downloaded By: [University of Washington] At: 18:07 13 March 2008

[58] L. Novotny, M.R. Beversluis, K.S. Youngworth, and T.G. Brown, Phys. Rev. Lett. **86**, 5251 (2001).
[59] B. Sick, B. Hecht, and L. Novotny, Phys. Rev. Lett. **85**, 4482 (2000).
[60] J. Wang and R. Richert, J. Chem. Phys. **120**, 11082 (2004).
[61] E. Mitscherlich, Ann. Chim. Phys. Paris **14**, 172 (1820).
[62] B. Kahr and R.W. Gurney, Chem. Rev. **101**, 893 (2001).
[63] A. Barbon, M. Bellinazzi, J.B. Benedict, M. Brustolon, S.D. Fleming, S.H. Jang, B. Kahr, and A.L. Rohl, Angew. Chem. Int. Ed. Engl. **43**, 5328 (2004).
[64] M. Bellinazzi, A. Barbon, B. Kahr, J.B. Benedict, and M. Brustolon, Phys. Chem. Chem. Phys. **8**, 379 (2006).
[65] J.R. Benedict, P.M. Wallace, P.J. Reid, S.H. Jang, and B. Kahr, Adv. Mater. **15**, 1068 (2003).
[66] K.L. Wustholz, B. Kahr, and P.J. Reid, J. Phys. Chem. B **109**, 16357 (2005).
[67] L.D. Bastin and B. Kahr, Tetrahedron **56**, 6633 (2000).
[68] R.W. Gurney, C.A. Mitchell, S. Ham, L.D. Bastin, and B. Kahr, J. Phys. Chem. B **104**, 878 (2000).
[69] B. Kahr, S. Lovell, and J.A. Subramony, Chirality **10**, 66 (1998).
[70] M. Kurimoto, B. Muller, W. Kaminsky, B. Kahr, and L.W. Jin, Molec, Cryst. Liquid Cryst. **389**, 1 (2002).
[71] S. Lovell, P. Subramony, and B. Kahr, J. Amer. Chem. Soc. **121**, 7020 (1999).
[72] G. Tammann, *Die chemischen und galvanischen Eigenschaften von Mischkristallreihen und ihre Atomverteilung*. (Leopold Voss, Leipzig, 1919).
[73] T. Bullard, J. Freudenthal, S. Avagyan, and B. Kahr, Faraday Disc. **136**, 231 (2007).
[74] T. Bullard, M. Kurimoto, S. Avagyan, S.H. Jang, and B. Kahr, ACA Trans. **39**, 62 (2004).
[75] Y. Okaya, Acta Crystallogr. **19**, 879 (1965).
[76] M. Rifani, Y.Y. Yin, D.S. Elliott, M.J. Jay, S.H. Jang, M.P. Kelley, L.D. Bastin, and B. Kahr, J. Amer. Chem. Soc. **117**, 7572 (1995).
[77] J. Michl and E.W. Thulstrup, *Spectroscopy with Polarized Light: Solute Alignment by Photoselection, in Liquid Crystals, Polymers, and Membranes*, 2nd ed. (VCH, New York, 1995).
[78] J.Y.P. Butter, B.R. Crenshaw, C. Weder, and B. Hecht, Chem. Phys. Chem. **7**, 261 (2006).
[79] D. Axelrod, Biophys. J. **26**, 557 (1979); H. Yang, J. Phys. Chem. A **111**, 4987 (2007).
[80] R.J. Pfab, J. Zimmermann, C. Hettich, I. Gerhardt, A. Renn, and V. Sandoghdar, Chem. Phys. Lett. **387**, 490 (2004).
[81] N.F. van Hulst, J.A. Veerman, M.F. Garcia-Parajo, and L. Kuipers, J. Chem. Phys. **112**, 7799 (2000).
[82] T. Ha, T. Enderle, D.S. Chemla, P.R. Selvin, and S. Weiss, Phys. Rev. Lett. **77**, 3979 (1996).
[83] M.A. Weber, F. Stracke, and A.J. Meixner, Cytometry **36**, 217 (1999).
[84] A. Bloess, Y. Durand, M. Matsushita, J. Schmidt, and E.J.J. Groenen, Chem. Phys. Lett. **344**, 55 (2001).
[85] A. Bloess, Y. Durand, M. Matsushita, R. Verberk, E.J.J. Groenen, and J. Schmidt, J. Phys. Chem. A **105**, 3016 (2001).
[86] C.R. Viteri, J.W. Gilliland, and W.T. Yip, J. Amer. Chem. Soc. **125**, 1980 (2003).
[87] S.A. Empedocles, R. Neuhauser, and M.G. Bawendi, Nature **399**, 126 (1999).
[88] C.G. Hubner, V. Ksenofontov, F. Nolde, K. Mullen, and T. Basche, J. Chem. Phys. **120**, 10867 (2004).
[89] W. Schroeyers, R. Vallee, D. Patra, J. Hofkens, S. Habuchi, T. Vosch, M. Cotlet, K. Mullen, J. Enderlein, and F.C. De Schryver, J. Amer. Chem. Soc. **126**, 14310 (2004).
[90] C.A. Werley and W.E. Moerner, J. Phys. Chem. B **110**, 18939 (2006).
[91] K.L. Wustholz, E.D. Bott, C.M. Isborn, X. Li, B. Kahr, and P.J. Reid, J. Phys. Chem. C **111**, 9146 (2007).
[92] N. Kejalakshmy and K. Srinivasan, J. Phys. D. **36**, 1778 (2003).
[93] T. Bullard, K.L. Wustholz, M. Robertson, P.J. Reid, and B. Kahr, J. Amer. Chem. Soc. in preparation, (2008).
[94] W.T. Yip, D.H. Hu, J. Yu, D.A. Vanden Bout, and P.F. Barbara, J. Phys. Chem. A. **102**, 7564 (1998).
[95] F. Kulzer, S. Kummer, T. Basche, and C. Brauchle, J. Infor. Rec. **22**, 567 (1996).
[96] J.A. Veerman, M.F. Garcia-Parajo, L. Kuipers, and N.F. van Hulst, Phys. Rev. Lett. **83**, 2155 (1999).
[97] J. Bernard, L. Fleury, H. Talon, and M. Orrit, J. Chem. Phys. **98**, 850 (1993).
[98] F. Kohn, J. Hofkens, R. Gronheid, M. Van der Auweraer, and F.C. De Schryver, J. Phys. Chem. A **106**, 4808 (2002).
[99] I.H. Chung and M.G. Bawendi, Phys. Rev. B **70**, 165304 (2004).
[100] G. Margolin, V. Protasenko, and M. Kuno, in *Advances in Chemical Physics*, edited by S.A. Rice (John Wiley and Sons, Hoboken, New Jersey, 2006), Vol. 133, p. 327.
[101] S.A. Empedocles and M.G. Bawendi, J. Phys. Chem. B **103**, 1826 (1999).
[102] M. Kuno, D.P. Fromm, A. Gallagher, D.J. Nesbitt, O.I. Micic, and A.J. Nozik, Nano Lett. **1**, 557 (2001).
[103] M. Kuno, D.P. Fromm, H.F. Hamann, A. Gallagher, and D.J. Nesbitt, J. Chem. Phys. **112**, 3117 (2000).
[104] M. Kuno, D.P. Fromm, H.F. Hamann, A. Gallagher, and D.J. Nesbitt, J. Chem. Phys. **115**, 1028 (2001).
[105] M. Kuno, D.P. Fromm, S.T. Johnson, A. Gallagher, and D.J. Nesbitt, Phys. Rev. B **67**, 125304 (2003).
[106] D.J. Nesbitt, Abstr. Pap. Amer. Chem. Soc. **225**, 456 (2003).
[107] K.T. Shimizu, R.G. Neuhauser, C.A. Leatherdale, S.A. Empedocles, W.K. Woo, and M.G. Bawendi, Phys. Rev. B **63**, 205316 (2001).

Downloaded By: [University of Washington] At: 18:07 13 March 2008

[108] F.D. Stefani, W. Knoll, M. Kreiter, X. Zhong, and M.Y. Han, Phys. Rev. B **72**, 125304 (2005).
[109] F.D. Stefani, X.H. Zhong, W. Knoll, M.Y. Han, and M. Kreiter, New J. Phys. **7**, 197 (2005).
[110] A. Issac, C. von Borczyskowski, and F. Cichos, Phys. Rev. B **71**, 161302 (2005).
[111] R. Verberk, A.M. van Oijen, and M. Orrit, Phys. Rev. B **66**, 233202 (2002).
[112] J. Tang and R.A. Marcus, J. Chin. Chem. Soc. **53**, 1 (2006).
[113] S.A. Blanton, A. Dehestani, P.C. Lin, and P. Guyot-Sionnest, Chem. Phys. Lett. **229**, 317 (1994).
[114] S.A. Blanton, M.A. Hines, and P. Guyot-Sionnest, App. Phys. Lett. **69**, 3905 (1996).
[115] S.A. Empedocles, D.J. Norris, and M.G. Bawendi, Phys. Rev. Lett. **77**, 3873 (1996).
[116] J. Tittel, W. Gohde, F. Koberling, T. Basche, A. Kornowski, H. Weller, and A. Eychmuller, J. Phys. Chem. B. **101**, 3013 (1997).
[117] W.P. Ambrose, P.M. Goodwin, J.C. Martin, and R.A. Keller, Phys. Rev. Lett. **72**, 160 (1994).
[118] M. Haase, C.G. Hubner, E. Reuther, A. Herrmann, K. Mullen, and T. Basche, J. Phys. Chem. B. **108**, 10445 (2004).
[119] J. Hofkens, T. Vosch, M. Maus, F. Kohn, M. Cotlet, T. Weil, A. Herrmann, K. Mullen, and F.C. De Schryver, Chem. Phys. Lett. **333**, 255 (2001).
[120] J.P. Hoogenboom, E. van Dijk, J. Hernando, N.F. van Hulst, and M.F. Garcia-Parajo, Phys. Rev. Lett. **95**, 097401 (2005).
[121] I.S. Osad'ko, J. Exp. Theor. Phys. **96**, 617 (2003).
[122] J. Schuster, F. Cichos, and C. von Borczyskowski, Appl. Phys. Lett. **87**, 051915 (2005).
[123] J. Schuster, F. Cichos, and C. von Borczyskowski, Opt. Spec. **98**, 712 (2005).
[124] K.D. Weston and S.K. Buratto, J. Phys. Chem. A **102**, 3635 (1998).
[125] E.K.L. Yeow, S.M. Melnikov, T.D.M. Bell, F.C. De Schryver, and J. Hofkens, J. Phys. Chem. A **110**, 1726 (2006).
[126] R. Zondervan, F. Kulzer, S.B. Orlinskii, and M. Orrit, J. Phys. Chem. A **107**, 6770 (2003).
[127] J.P. Hoogenboom, J. Hernando, E. van Dijk, N.F. van Hulst, and M.F. Garcia-Parajo, Chem. Phys. Chem. **8**, 823 (2007).
[128] H.P. Lu and X.S. Xie, Nature **385**, 143 (1997).
[129] F. Stracke, C. Blum, S. Becker, K. Mullen, and A.J. Meixner, Chem. Phys. Chem. **6**, 1242 (2005).
[130] P. Tchenio, A.B. Myers, and W.E. Moerner, J. Lumines. **56**, 1 (1993).
[131] T. Christ, F. Kulzer, P. Bordat, and T. Basche, Angew. Chem. Int. Ed. Engl. **40**, 4192 (2001).
[132] J. Yu, D.H. Hu, and P.F. Barbara, Science **289**, 1327 (2000).
[133] P. Tinnefeld, J. Hofkens, D.P. Herten, S. Masuo, T. Vosch, M. Cotlet, S. Habuchi, K. Mullen, F.C. De Schryver, and M. Sauer, Chem. Phys. Chem. **5**, 1786 (2004).
[134] N.J. Turro, *Modern Molecular Photochemistry* (University Science Books, Sausalito, California, 1991).
[135] C.A. Mitchell, R.W. Gurney, S.H. Jang, and B. Kahr, J. Amer. Chem. Soc. **120**, 9726 (1998).
[136] J.N. Clifford, T.D.M. Bell, P. Tinnefeld, M. Heilemann, S.M. Melnikov, J.I. Hotta, M. Sliwa, P. Dedecker, M. Sauer, J. Hofkens, and E.K.L. Yeow, J. Phys. Chem. B **111**, 6987 (2007).
[137] J.P. Hoogenboom, W.K. den Otter, and H.L. Offerhaus, J. Chem. Phys. **125**, 204713 (2006).
[138] G. Margolin and E. Barkai, J. Chem. Phys. **121**, 1566 (2004).
[139] J. Tang and R.A. Marcus, J. Chem. Phys. **123**, 204511 (2005).
[140] J. Tang and R.A. Marcus, Phys. Rev. Lett. **95**, 107401 (2005).
[141] J.P. Bouchaud and A. Georges, Phys. Reports **195**, 127 (1990).
[142] M.J. Frisch, G.W. Trucks, H.B. Schlegel, G.E. Scuseria, M.A. Robb, J.R. Cheeseman, J.J.A. Montgomery, T. Vreven, K.N. Kudin, J.C. Burant, J.M. Millam, S.S. Iyengar, *et al.* (Gaussian, Inc, Wallingford, CT, 2004).
[143] F. Kulzer, S. Kummer, R. Matzke, C. Brauchle, and T. Basche, Nature **387**, 688 (1997).
[144] M. Orrit, J. Bernard, and R.I. Personov, J. Phys. Chem. **97**, 10256 (1993).
[145] K.L. Wustholz, E.D. Bott, B. Kahr, and P.J. Reid, J. Phys. Chem. C Accepted, (2008).